

1969

Weight optimization of reactor shielding using transmission matrix methods

William Dale Leech
Iowa State University

Follow this and additional works at: <https://lib.dr.iastate.edu/rtd>

 Part of the [Nuclear Engineering Commons](#), and the [Oil, Gas, and Energy Commons](#)

Recommended Citation

Leech, William Dale, "Weight optimization of reactor shielding using transmission matrix methods " (1969). *Retrospective Theses and Dissertations*. 4125.
<https://lib.dr.iastate.edu/rtd/4125>

This Dissertation is brought to you for free and open access by the Iowa State University Capstones, Theses and Dissertations at Iowa State University Digital Repository. It has been accepted for inclusion in Retrospective Theses and Dissertations by an authorized administrator of Iowa State University Digital Repository. For more information, please contact digirep@iastate.edu.

70-13,605

LEECH, William Dale, 1944-
WEIGHT OPTIMIZATION OF REACTOR SHIELDING USING
TRANSMISSION MATRIX METHODS.

Iowa State University, Ph.D., 1969
Engineering, nuclear

University Microfilms, Inc., Ann Arbor, Michigan

THIS DISSERTATION HAS BEEN MICROFILMED EXACTLY AS RECEIVED

WEIGHT OPTIMIZATION OF REACTOR SHIELDING
USING TRANSMISSION MATRIX METHODS

by

William Dale Leech

A Dissertation Submitted to the
Graduate Faculty in Partial Fulfillment of
The Requirements for the Degree of
DOCTOR OF PHILOSOPHY

Major Subject: Nuclear Engineering

Approved:

Signature was redacted for privacy.

In Charge of Major Work

Signature was redacted for privacy.

Head of Major Department

Signature was redacted for privacy.

Dean of Graduate College

Iowa State University
Ames, Iowa

1969

TABLE OF CONTENTS

	Page
INTRODUCTION	1
GENERAL THEORY	5
Primary Gamma Rays	5
The transmission matrix method	6
Secondary Gamma Rays	12
Fast and Thermal Neutrons	16
Summary and Example	19
PROCEDURE	23
Transmission Matrix Energy Groups and Angular Expansion	26
Input Parameters	37
Weight Optimization	39
RESULTS	41
Slab Shields	41
Cylindrical Shields	51
Fast Reactor Shields	54
Input Parameter Variation	56
SUMMARY OF RESULTS	59
SUGGESTIONS FOR FURTHER STUDY	62
LITERATURE CITED	64
ACKNOWLEDGMENTS	66

INTRODUCTION

A technique by which a reduced weight shield for a nuclear reactor can be obtained has obvious uses under certain circumstances. For a reactor which is to be launched into space the weight of the shielding is of primary importance. Reducing the weight of the shield can result in an equal increase in the effective payload which is launched. Mobile reactors, which are designed to be moved into a remote area and then assembled quickly to produce electrical power, also need to be as light as possible to facilitate shipping and assembly. One of the obvious methods of reducing weight is by the proper design of the shield. For large stationary power reactors minimum weight shielding ususally is less desirable than minimum cost shielding. In many cases, however, decreased weight implies decreased cost of the shielding.

The different types of radiation coming from a reactor core necessitate combining light and heavy materials to form the reactor shield. The light materials, usually containing a large amount of hydrogen, are used to thermalize the fast neutrons coming from the core. Thermalization aids in the capture of neutrons by the materials in the shield. The heavy materials are required to attenuate gamma radiation from the reactor core as well as secondary gamma rays produced by the capture of the thermal neutrons in the shield.

It should be noted that secondary gammas are also formed by inelastic scattering of fast neutrons in the shield but this effect is usually small in comparison to the gamma rays produced by thermal neutron capture.

Work has been done on optimum shield design by Hurwitz (5), Troubetzkoy (12), and Blizard (1). They assumed arbitrary gamma ray and neutron distributions in the shield, and used calculus of variation techniques to develop equations. The solution of which yielded the proper volume ratios of the light to heavy materials, as a function of position, for a minimum weight shield. Sasse (10), using diffusion-removal theory for the neutrons and buildup factors for the primary gamma rays, developed equations which yielded similar results to Hurwitz and Troubetzkoy for a lead-water spherical shield.

These results, while useful from a theoretical point of view, have doubtful practical application because of the nature of their results. It is impractical, if not impossible, to build a shield with a constantly varying volume percent of heavy material dispersed in a light material. For example, the cost of building a reactor shield of concrete and iron where the volume percent of iron in the concrete varies with location would undoubtedly be higher than a conventional nuclear reactor shield even though the conventional shield would be heavier.

One would not expect the cost to increase drastically if layers of light and heavy materials were used. In this case construction difficulties would be held to a minimum and a significant weight reduction would yield a cost reduction. This was the type of shield studied in this investigation. This type of shield has also been studied by Mynatt (7, 8) for the SNAP reactor program. A computer code, ASOP, was developed which produced a twenty-five percent reduction in shield weight by proper lamination of the tungsten-lithium hydride shield.

The optimization in this investigation has been carried out by determining the weight of various primary shield configurations and then by searching for a minimum weight. The shield configuration was determined by the thicknesses, location, and number of the iron, lead, and water slabs that make up the primary shield. The dose at the outside of the shield was held constant for the various configurations so that a meaningful comparison of the weights could be accomplished.

The fast neutron dose was obtained by using the removal cross section concept in diffusion theory. The use of this technique constrained the shield configurations to have a minimum of 40 cm of water following the last slab of heavy material. The thermal neutron distribution in the shield was obtained from the two group diffusion equations using Fermi age theory for the slowing down of the fast neutrons.

The primary and secondary gamma rays were treated by transmission matrix techniques as outlined by Boulette (2) and Yarmush (14).

Studies were conducted on iron-water slab shields, lead-water slab shields, iron-water cylindrical shields, and lead-water cylindrical shields. Fast reactor shields as well as thermal reactor shields were studied. Finally in an attempt to develop a better feeling for the reaction mechanisms which control the weight of the shield, the input quantities of thermal neutrons and primary gamma rays were varied and the changes in the dose at the outside of the shield were studied.

GENERAL THEORY

In any reactor the purpose of the shield is to reduce radiation produced by the reactor to a tolerable level. The radiation to be attenuated is usually divided into four categories; fast neutrons, thermal neutrons, primary gamma rays, and secondary gamma rays. In the following sections each of these categories will be discussed.

Primary Gamma Rays

Primary gamma rays are those which are produced in the reactor through the fission process, decay of fission products, radiative capture by materials in the core, and inelastic scatter of fast neutrons. These gamma rays which have different energies and directions of travel leave the reactor core and enter the shield. Many techniques have been developed to determine the transport of these gamma rays through a material. Some of these techniques are as follows: Monte Carlo, S_n , discrete S_n , invariant imbedding, and transmission matrix techniques. All of these methods involve numerical solutions. The transmission matrix method was chosen for this particular investigation because it allows the investigation of many shield configurations with a minimum of computer time.

The transmission matrix method

A one-dimensional homogeneous slab of thickness t is represented in Figure 1.

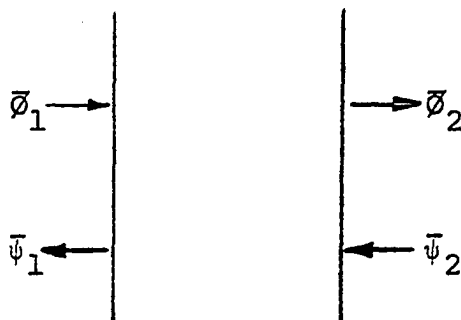


Figure 1. Slab shield

Here $\bar{\phi}_1$ and $\bar{\psi}_1$ are the incoming and outgoing distributions in energy and angle on the left face of the slab and $\bar{\phi}_2$ and $\bar{\psi}_2$ are the outgoing and incoming distributions on the right face. For shielding work $\bar{\phi}_2$ is the important parameter if the radiation is incident from the left. For the case of primary gamma rays where no sources are present in the slab there exists a linear operator $H(t)$ such that

$$\begin{bmatrix} \bar{\phi}_2 \\ \bar{\psi}_2 \end{bmatrix} = H(t) \begin{bmatrix} \bar{\phi}_1 \\ \bar{\psi}_1 \end{bmatrix}, \quad (1)$$

where

$$H(t) = \begin{bmatrix} T - RT^{-1}R & RT^{-1} \\ -T^{-1}R & T^{-1} \end{bmatrix} . \quad (2)$$

Here T is the transmission operator and R is the reflection operator while R^{-1} and T^{-1} are the inverse operators. The transmission and reflection operators for a homogeneous slab of thickness t are obtained from the transmission and reflection functions of an infinitesimally thin slab of the same material. The transmission and reflection functions are written in terms of the basic cross sections of the material. Once the transmission and reflections operators for a slab have been determined these operators can be used to transform an incoming vector in angle and energy into an outgoing vector in angle and energy. For example, in shielding work one is concerned with $\bar{\phi}_2$. From Equations 1 and 2 one obtains

$$\bar{\phi}_2 = [T - RT^{-1}R] \bar{\phi}_1 + [RT^{-1}] \bar{\psi}_1 . \quad (3)$$

Boulette (2) has shown that the reflection operator is much smaller than the transmission operator. This information plus the fact that $\bar{\psi}_1$ would be much less than $\bar{\phi}_1$ for a shield with the reactor situated on the left implies

$$\bar{\phi}_2 \approx T \bar{\phi}_1 . \quad (4)$$

It should be emphasized that neglecting R and $\bar{\psi}_1$, while

valid for gamma ray problems, is not valid for neutron studies.

If the shield is made up of n adjacent laminae with individual operators given by H_i where i designates the i th lamina from the left, then the H operator for the system is

$$H = H_n H_{n-1} \dots H_2 H_1 \quad . \quad (5)$$

This implies the H operator is an exponential in t and can be written as

$$H(t) = \exp[-Wt] \quad , \quad (6)$$

where W is a constant operator.

For a slab of thickness $t_1 + t_2$ the transmission operator can be written as

$$T(t_1 + t_2) = T(t_2)[I - R(t_1)R(t_2)] T(t_1) \quad , \quad (7)$$

where $T(t_2)$ and $T(t_1)$ are the transmission operators for slabs of thicknesses t_2 and t_1 respectively. $R(t_1)$ and $R(t_2)$ are the corresponding reflection operators and I is the unit operator (9). Again using the assumption that the reflection operators are small when compared to the transmission operators one obtains

$$T(t_1 + t_2) = T(t_2)T(t_1) \quad . \quad (8)$$

In general one obtains for a slab of thickness nt

$$T(nt) = [T(t)]^n \quad . \quad (9)$$

For a shield composed of n laminae all of thickness t and an input flux in angle and energy, the output flux in angle and energy is approximately given by

$$\bar{\phi}_2 = [T(t)]^n \bar{\phi}_1 \quad (10)$$

The transmission and reflection operators can be expressed as integral operators in energy and angle. The angular dependence is expressed in terms of a polynomial expansion of the cosine of the angle between the slab normal and the direction of travel of the gamma ray. The energy dependence is approximated by dividing the energy range into several groups and assuming the distribution of the gamma rays is constant within each group. The integral operators are then transformed to matrix operators by numerical integration.

The transmission matrix T is lower block triangular in form. Each block refers to an energy group, and the elements in each block transform the incoming angular distribution into an outgoing distribution. All blocks above the diagonal are zero because it is impossible for a gamma ray to scatter from a low energy group to a higher energy group. In this investigation, the angular dependence was approximated by a third-order half-range Legendre polynomial expansion. Thus, the first column of the block column of the transmission matrix gives the energy and angular distributions of the

transmitted flux due to an isotropic source in the upper-most group. The second column corresponds to source whose angular dependence is defined by the second half-range Legendre polynomial, $2\omega-1$. Similarly, the third column corresponds to a source whose angular dependence is defined by the third half-range Legendre polynomial, $6\omega^2 - 6\omega + 1$. In general, then, the first block column of the transmission matrix determines the transmitted flux vector due to a source in the upper energy group whose angular dependence is defined in the following manner:

$$S(\omega) = a(1) + b(2\omega - 1) + c(6\omega^2 - 6\omega + 1)$$

where a , b , and c are constants selected to describe the angular dependence of the source. For instance,

$a = 1, b = c = 0$ corresponds to an isotropic source and
 $a = 1/2 = b, c = 0$ corresponds to a cosine source.

The magnitude of the source is also controlled by these constants. For example,

$a = 10, b = c = 0$ is an isotropic source ten times the
 strength of an isotropic source given by the
 constants

$a = 1, b = c = 0$.

The second column of blocks determines the transmitted flux vector for a source in the second energy group and so on for

the rest of the columns.

From this information $\bar{\phi}_2$ in Equation 10 can be determined. The transmission matrix, T, for a thickness t is first calculated. The source vector, $\bar{\phi}_1$, is written so that the constants a, b, and c give the desired angular dependence and magnitude for each energy group. The vector $\bar{\phi}_1$ is then multiplied times T yielding a vector whose constants determine the magnitude and angular distribution, for each of the energy groups, of the flux at a distance t into the material. This new vector is then multiplied by T yielding a similar vector for a position 2t into the material. This process is repeated n times and finally an output vector for the entire slab is obtained. The orthogonality property of the half-range Legendre polynomials greatly simplifies the interpretation of the output flux, since the first coefficient in each energy group of the output vector is the total energy output in that group.

It would, of course, be possible to calculate the transmission matrix for the entire slab of thickness nt and thus avoid the repetition and approximations used in the above method. The method outlined has the advantage of being able to determine the output flux for various slab thicknesses by simply varying the number of repetitions. This process is much quicker, in terms of computer time, than calculating the transmission matrices for all the slab thickness to be

studied in the optimization procedure to determine a minimum weight shield.

Secondary Gamma Rays

Secondary gamma rays are produced in the shield through the radiative capture of thermal neutrons. Other sources of secondary gamma rays, such as inelastic scatter of fast neutrons, will be ignored in this investigation since they are usually of minor importance when compared to thermal neutron capture. Secondary gamma rays are produced in the shield at any location where thermal neutrons are present and thus the source of these gamma rays is distributed through the shield. To apply the transmission matrix operator to a distributed source the source must be approximated by a finite number of infinite plane sources. The following development presents one method by which a distributed secondary source can be approximated by a finite number of infinite sources.

One again considers a homogeneous slab of thickness nt composed of n laminae all of thickness t . The distributed source in the first lamina is replaced by an equivalent plane source at the right edge of the first lamina. The resulting flux exiting from the right side of the total slab from this plane source is

$$\bar{\phi}_{r1} = T^{n-1} \bar{\phi}_{s1} \quad (11)$$

where

$\bar{\phi}_{s1}$ = equivalent plane source at right edge of first lamina

$\bar{\phi}_{r1}$ = outcoming vector due to the above source

T = transmission matrix for the homogeneous slab of thickness t.

The second lamina is treated in the same manner and a similar result is obtained

$$\bar{\phi}_{r2} = [T^{n-2}] \bar{\phi}_{s2} \quad (12)$$

Repeating this process for each of the laminae and summing the outcoming flux from each of the plane sources to obtain a total outcoming flux vector one obtains

$$\bar{\phi}_{TR} = \sum_{i=1}^n [T^{n-i}] \bar{\phi}_{si} \quad (13)$$

where

i = the number of the lamina

$\bar{\phi}_{TR}$ = total outcoming flux vector from the secondary gamma rays.

Secondary gammas produced by thermal neutron captures are produced isotropically. Thus, the number of secondary gammas produced in a thickness t having energy E' and traveling in the direction such that the cosine of the angle with

the slab normal is ω' is given by

$$\phi(\omega', E) = 1/2 \int_0^t K \Phi_{th}(t') \sigma_{n,\gamma} f(E') dt' \quad , \quad (14)$$

where Φ_{th} is the thermal neutron distribution as a function of the distance t , $\sigma_{n,\gamma}$ is the macroscopic thermal neutron capture cross section, $f(E')$ is the secondary gamma energy spectrum, and K is the number of secondary gammas produced per thermal neutron capture (1).

This source is approximated by an infinite plane source of gammas located at an effective position in the slab, t_{eff} , which is weighted with the secondary gamma source $\phi_s(\omega', E')$.

Thus

$$t_{eff} = \frac{1/2 \int_0^t t' K \Phi_{th}(t') \sigma_{n,\gamma} f(E') dt'}{1/2 \int_0^t K \Phi_{th}(t') \sigma_{n,\gamma} f(E') dt'} \quad (15)$$

$$= \frac{\int_0^t t' \Phi_{th}(t') dt'}{\int_0^t \Phi_{th}(t') dt'} \quad . \quad (16)$$

To take advantage of the property of the T operator indicated in Equation 13 the infinite plane secondary gamma source must be adjusted so that it coincides with the face of a lamina, in this case, the interface between the first

and second laminae. The source adjustment involves two factors. First, there is the simple exponential attenuation factor, $\exp(-(t-t_{\text{eff}})/\lambda_g)$ where λ_g is the average mean free path for the g^{th} gamma energy group, and secondly, there is the distortion of the angular dependence of the flux. With the assumption that there are no scattering events taking place while the gammas travel through the thickness $t - t_{\text{eff}} < 1$ mean free path, the angular dependence is transformed from isotropic to cosine in nature. Thus, the adjusted source at the interface is

$$\phi_{\text{adj}}(\omega', E') = \omega' \exp[(t_{\text{eff}} - t)/\lambda_g] \phi_s(\omega', E') \quad , \quad (17)$$

or in terms of the half-range Legendre polynomials,

$$\phi_{\text{adj}}(\omega', E') = 1/2[1 + (2\omega' - 1)] \exp[(t_{\text{eff}} - t)/\lambda_g] \phi_s(\omega', E') \quad . \quad (18)$$

Substituting the expression for $\phi_s(\omega', E')$ into Equation 14, the coefficients a , b , and c of the Legendre polynomials for each group become

$$a_g = b_g / 4 \sigma_{n,\gamma} f'_g \exp[-(t-t_{\text{eff}})/\lambda_g] \int_0^t \phi_{\text{th}}(t') dt' \quad (19)$$

$$c = 0 \quad ,$$

where f'_g is the summation of the product of the number of gamma rays produced per thermal neutron capture and the energy at which they are produced. This summation is carried out for all gammas emitted in the g^{th} energy group.

These coefficients for each energy group specify the equivalent plane source used for the distributed secondary gamma source in the first lamina. For the equivalent plane sources for the other laminae it is necessary only to change the limits of integration in Equations 16 and 19.

Boulette (2) carried out an investigation similar to this and found that the distributed source could be approximated, to a good degree of accuracy, by equivalent plane sources if the individual laminae are no more than one mean free path in thickness. Thus, using Equations 13, 16, and 19 the outgoing gamma flux vector from the secondary gamma rays produced in a slab of material of thickness nt can be determined once the thermal neutron flux distribution is known.

Fast and Thermal Neutrons

There are numerous methods available to determine the thermal and fast neutron flux in a reactor shield. Some of these methods are multigroup diffusion theory, multigroup solution of the transport equation using any one of a number of techniques already mentioned for the gamma ray penetration problem, and the removal cross section method (3). The removal cross section concept was used to calculate the fast neutron dose leaving the shield.

The removal cross section concept may be used when a

thin slab of material of thickness z is followed by a slab of water of thickness y of at least 40 cm. The 40 cm of water are required to insure that fast neutrons which undergo inelastic scattering in the heavy material are further slowed down and captured in the water. The major contribution to the dose after 40 cm of water is due to neutrons in the energy range 6-8 MeV. This is caused by the increasing penetrability of the neutrons and a decreasing proportion of them in the fission spectrum as the neutron energy is increased. The flux observed at the outside of the shield when a fission spectrum neutron source impinges on the heavy material is

$$\Phi_f(z+y) = e^{-\Sigma_r z} \Phi_{f_{H_2O}}(y) \quad , \quad (20)$$

where

$\Phi_f(z+y)$ = fast neutron flux at position $(z+y)$

Σ_r = removal cross section for the heavy material

$\Phi_{f_{H_2O}}$ = fast flux at position y if only water were present.

In this investigation an experimental kernel was used for the fast neutron distribution in the water (3)

$$\Phi_{f_{H_2O}}(y) = \Phi_f(0) [Ae^{-ay} + (1-A)e^{-by}] \quad , \quad (21)$$

where

$$\phi_f(0) = \text{fast flux at } y = 0$$

$$A = 0.892$$

$$a = 0.129$$

$$b = 0.091.$$

Thus the fast flux at the distance $(z+y)$ is

$$\bar{\phi}_f(z+y) = \bar{\phi}_f(0) e^{-\Sigma_r z} [Ae^{-ay} + (1-A)e^{-by}] \quad . \quad (22)$$

The thermal neutron distribution for the various slab configurations was obtained by numerical solution of the two group diffusion equations (6)

$$D_{f,i} \nabla^2 \bar{\phi}_{f,i} - \frac{\bar{\phi}_{f,i} D_{f,i}}{\tau_i} = 0 \quad (23)$$

$$D_{th,i} \nabla^2 \bar{\phi}_{th,i} - \bar{\phi}_{th,i} \Sigma_{th,i} + \frac{P_i \bar{\phi}_{f,i} D_{f,i}}{\tau_i} = 0 \quad , \quad (24)$$

where

$D_{f,i}, D_{th,i}$ = diffusion coefficients for the fast and thermal neutrons respectively for the i^{th} material

τ_i = Fermi age for the i^{th} material

$\Sigma_{th,i}$ = capture cross section for thermal neutrons of the i^{th} material

P_i = resonance escape probability for the i^{th} material

$\Phi_{f,i}$, $\Phi_{th,i}$ = fast and thermal flux respectively for the i^{th} material.

The usual boundary conditions of continuity of current and flux are used as well as the input values of fast and thermal flux.

From the numerical solution of the thermal neutron flux distribution across the shield the integrations indicated in Equations 16 and 19 are carried out numerically for each lamina. Thus all of the terms in Equation 19 are now known and the coefficients for the various secondary gamma ray infinite plane sources can be calculated. With these coefficients known the total dose exiting from the slab shield can be determined using Equation 10 for the primary gamma rays, Equation 13 for the secondary gamma rays, Equation 22 for the fast neutrons, and the solution to Equations 23 and 24 for the thermal neutrons.

Summary and Example

An example of the use of these equations and techniques for a specific shield follows. One wishes to determine the thickness of the water behind 10 cm of Pb needed to reduce the outcoming dose to a value D_0 (mrem/hr). The lead is considered to be made up of five laminae each 2 cm thick and

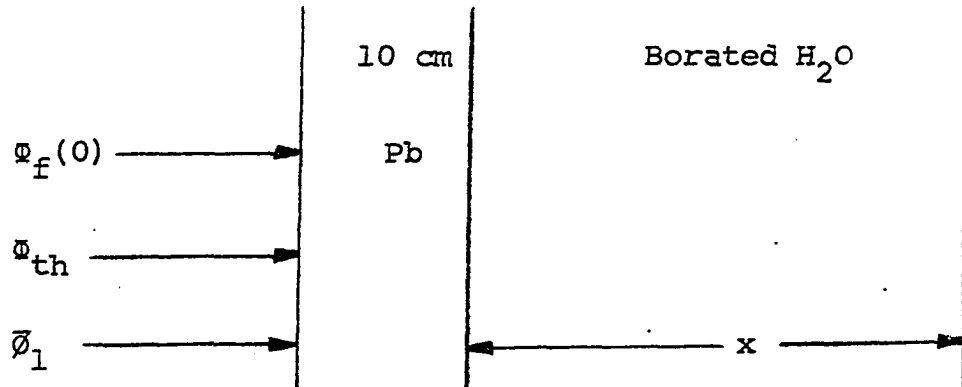


Figure 2. Example of a typical shield

the water made up of laminae each 9 cm thick. These thicknesses were chosen to satisfy the assumption made during the development of the secondary gamma ray equations that the laminae be less than one mean free path in thickness. Using a value for x that is known to be too large, Equations 23 and 24 are solved numerically to obtain the thermal flux distribution. The boundary conditions are specified so that the proper values of fast flux and thermal flux are obtained at the left boundary. Using this thermal flux distribution the following integrals are calculated for each laminae:

$$\int_0^T \phi_{th}(t') dt'$$

and

$$\int_0^T t' \phi_{th}(t') dt' ,$$

where

$$\begin{aligned} T &= 2 \text{ cm for the lead} \\ &= 9 \text{ cm for the H}_2\text{O}. \end{aligned}$$

Using these integrals t_{eff} for each lamina is calculated

$$t_{\text{eff}} = \frac{\int_0^T t' \Phi_{\text{th}}(t') dt'}{\int_0^T \Phi_{\text{th}}(t') dt'}$$

Using the above integrals and t_{eff} the Legendre polynomial coefficients for the equivalent plane sources of secondary gammas for each lamina are calculated from Equation 19

$$\begin{aligned} a_g = b_g &= 1/4 \sigma_{n,\gamma} f'_g [\exp[(t_{\text{eff}} - T)/\lambda_f]] \int_0^T \Phi_{\text{th}}(t') dt' \\ c_g &= 0 \end{aligned}$$

These coefficients specify the equivalent plane sources, Φ_{si} for each lamina. The total dose at a distance $9n$ cm into the water using Equations 10, 13, and 22 is

$$\begin{aligned} D(9n) &= \bar{D}_1 [T_{\text{Pb}}(2)]^5 [T_{\text{H}_2\text{O}}(9)]^n \bar{\Phi} \\ &+ \bar{D}_1 \sum_{i=1}^5 [T_{\text{Pb}}(2)]^{5-i} [T_{\text{H}_2\text{O}}(9)]^n \bar{\Phi}_{si} \\ &+ \bar{D}_1 \sum_{i=5}^n [T_{\text{H}_2\text{O}}(9)]^{n-i} \bar{\Phi}_{si} \end{aligned}$$

$$\begin{aligned}
& + D_2 \Phi_f(0) e^{-10\Sigma_r} [Ae^{-9an} - (1-A)e^{-9bn}] \\
& + D_3 \Phi_{th}(9n) \quad , \quad (25)
\end{aligned}$$

where

$T_{Pb}(2)$ = transmission matrix for 2 cm of Pb

$T_{H_2O}(9)$ = transmission matrix for 9 cm of H_2O

\bar{D}_1 = vector which transforms gamma energy vector
to a dose rate

D_2 = constant which converts fast neutron flux to
dose rate

D_3 = constant which transforms thermal neutron
flux to dose rate

$\bar{\phi}_1$ = primary gamma ray source vector

$\Phi_{th}(9n)$ = value of the thermal neutron flux as determined
by the solution to Equations 23 and 24

$\Phi_f(0)$ = input fast flux on the left side of the lead.

By using Equation 25 the dose rate is calculated at different distances into the water by increasing the value of n . When the outcoming dose rate falls below the desired value, D_0 , an interpolation is carried out to give the exact thickness of water needed to reduce the outcoming dose rate to D_0 .

PROCEDURE

In this chapter some assumptions that were made in the previous chapter will be checked by comparing the results with previously published calculations for an actual reactor.

Boulette (2) has shown the transmission matrix method can be expected to yield, to within a few percent, the outgoing gamma flux vector when an incoming flux vector is multiplied times the transmission matrix for a homogeneous slab of thickness t . He did not investigate if the output vector from a slab of thickness nt could be obtained by iterating across the slab using the transmission matrix for a slab of thickness t . In other words, it needs to be verified that Equation 10 is correct.

$$\vec{\phi}_2(nt) = [T(t)]^n \vec{\phi}_1$$

To check the validity of Equation 10 a test problem was carried out. Using a computer program, transmission matrices for water slabs 20, 40, 60, 80, 100, 140, and 200 cm thick were calculated. In these calculations five energy groups were used. Two different angular expansions were used. A three angle term expansion and five angle term expansion were used so that comparisons between the two could be made. The upper energy group was chosen as 2.001 to 1.999 MeV so that a 2.00 MeV source could be approximated. $\vec{\phi}_1$ was assumed as an isotropic source in this highest group. Using the transmission

matrix for the 20 cm slab, $\bar{\phi}_2$ was obtained at 40, 60, 80, 100, 140, and 200 cm by letting n take on the values 2, 3, 4, 5, and 10 in Equation 10. The buildup factor for each slab thickness was calculated from the output flux for both the iterated and non-iterated slabs. Shown in Figure 3 is the percent difference, for both angular expansions, in the buildup factors between the two methods.

The cause of the increasing difference with increasing thickness, or number of iterations, is believed to be caused by computer roundoff error. This conclusion is reached by noting that the curve in Figure 3 does not have the proper shape to be explained in terms of what is neglected by using Equation 10. In Equation 10 one does not consider gammas that are reflected from the second slab back into the first slab, which are then reflected back into and through the second slab. As the two slab thicknesses are increased the reflection mentioned above would be expected to increase, and one would expect the difference between the non-iterated and the iterated buildup factors to increase, as is shown in Figure 3. However, as the thickness continues to increase the difference between the methods should saturate to a constant value or possibly even decrease. This saturation of the percent difference is caused by the transmission of these reflected gammas through the second slab. The double reflection of those gammas which enter the second slab for the

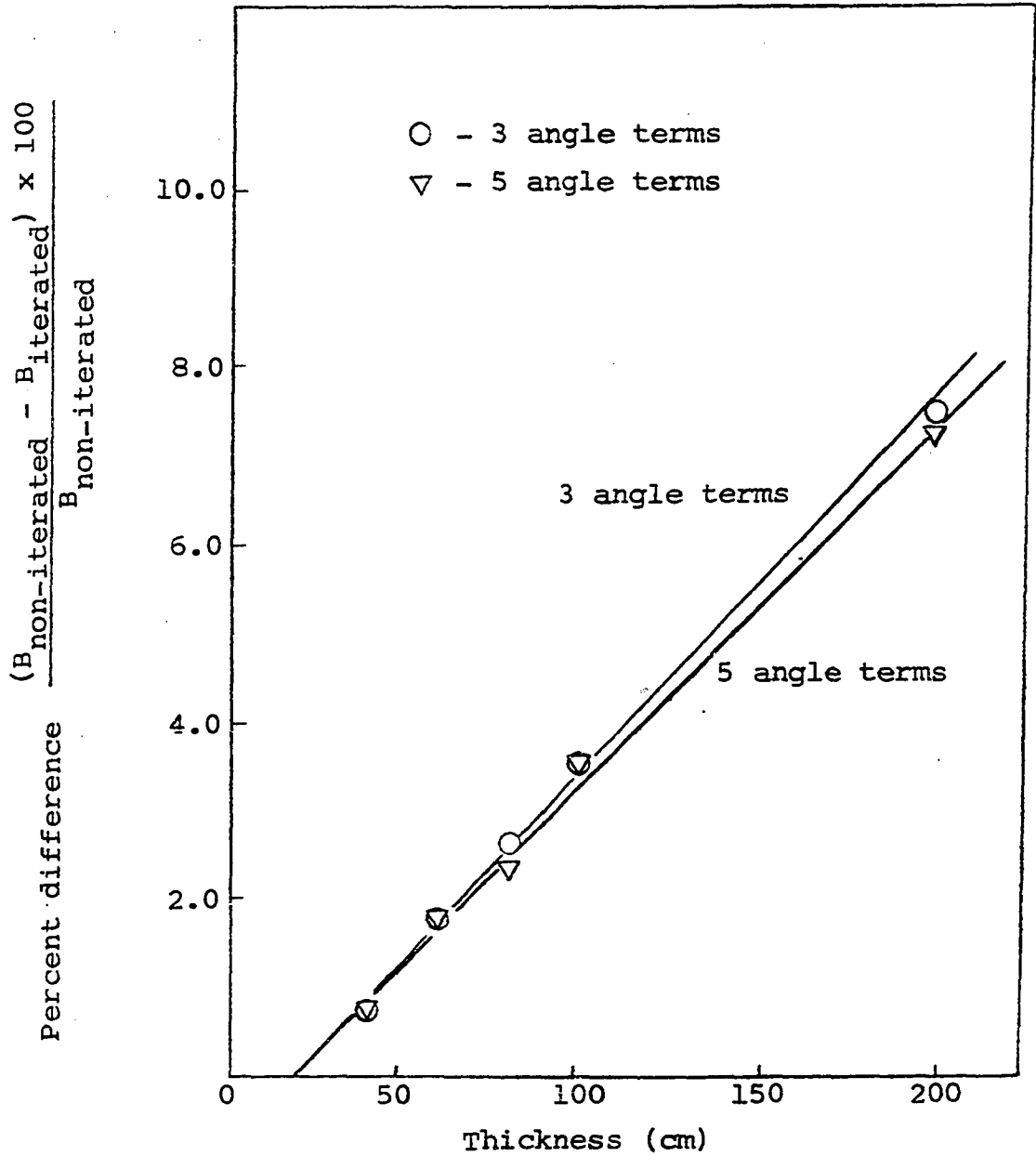


Figure 3. Buildup factor percent difference for iterated and non-iterated slabs

second time has greatly decreased their energy. At these low energies the attenuation coefficient of the water is very high and they do not penetrate far into the second slab. As the second slab thickness is increased fewer of them penetrate through this slab and thus the percent error in the buildup factor should saturate.

Transmission Matrix Energy Groups and Angular Expansion

To determine the number of angle terms needed the buildup factors mentioned earlier for the 20, 40, 60, 80, 100, 140, and 200 cm slabs were used. The percent difference in the buildup factors for the three term and five term angular expansions were calculated. Shown in Figure 4 is this percent difference as a function of slab thickness.

The cause of the oscillation up to 140 cm is most probably due to computer roundoff error and is insignificant. Above 140 cm the decrease in the curve is caused by the inability of the three-term expansion to represent the large amount of forward peaking of the flux. This develops in the higher energy groups as the slab thickness is increased. Since the buildup factor using three angle terms seems to be in error for thicker slabs, it was decided that the buildup factors obtained by the iterative technique for three angle term expansion should be compared to the non-iterated five

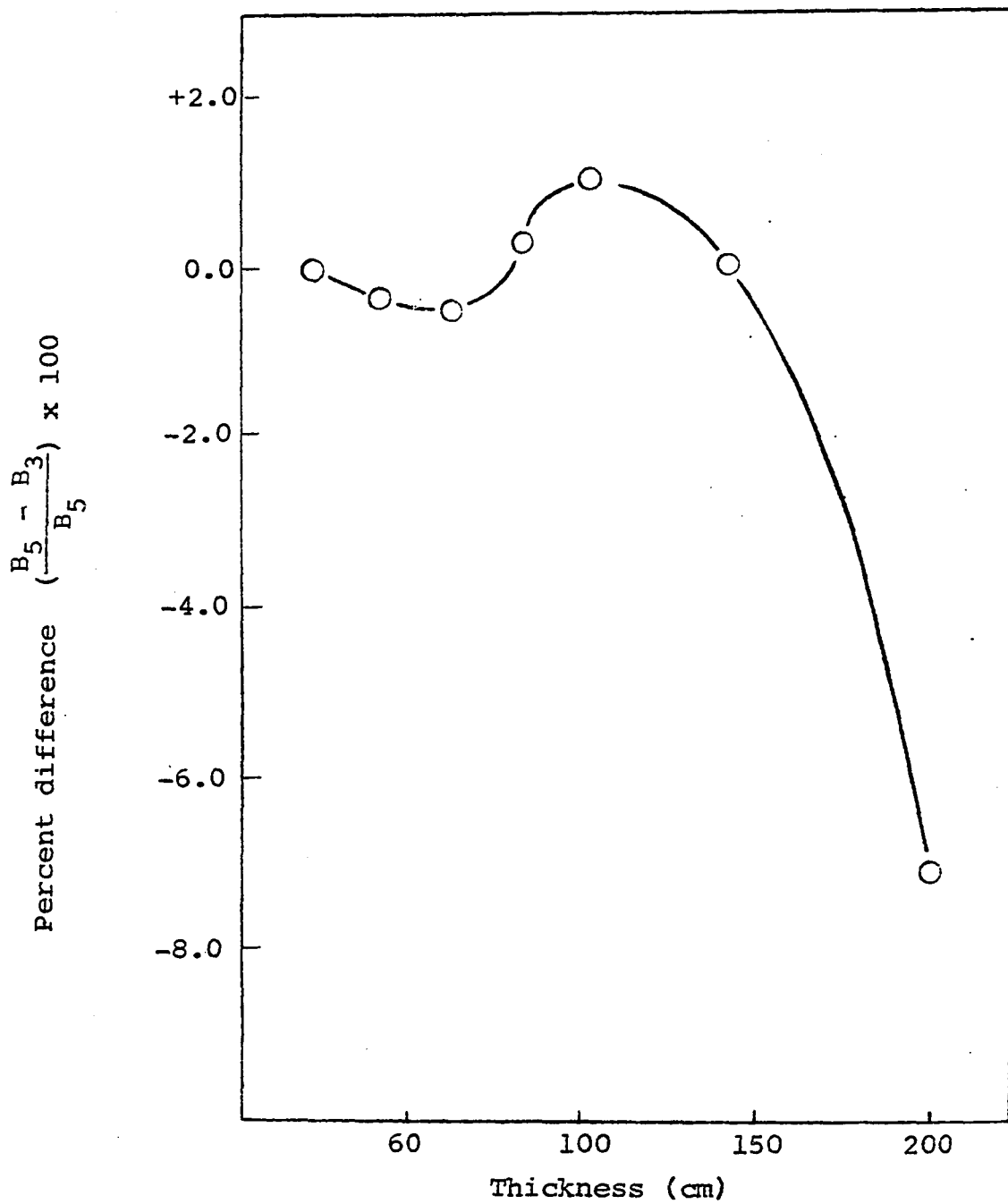


Figure 4. Percent difference in buildup factor for different angular expansions

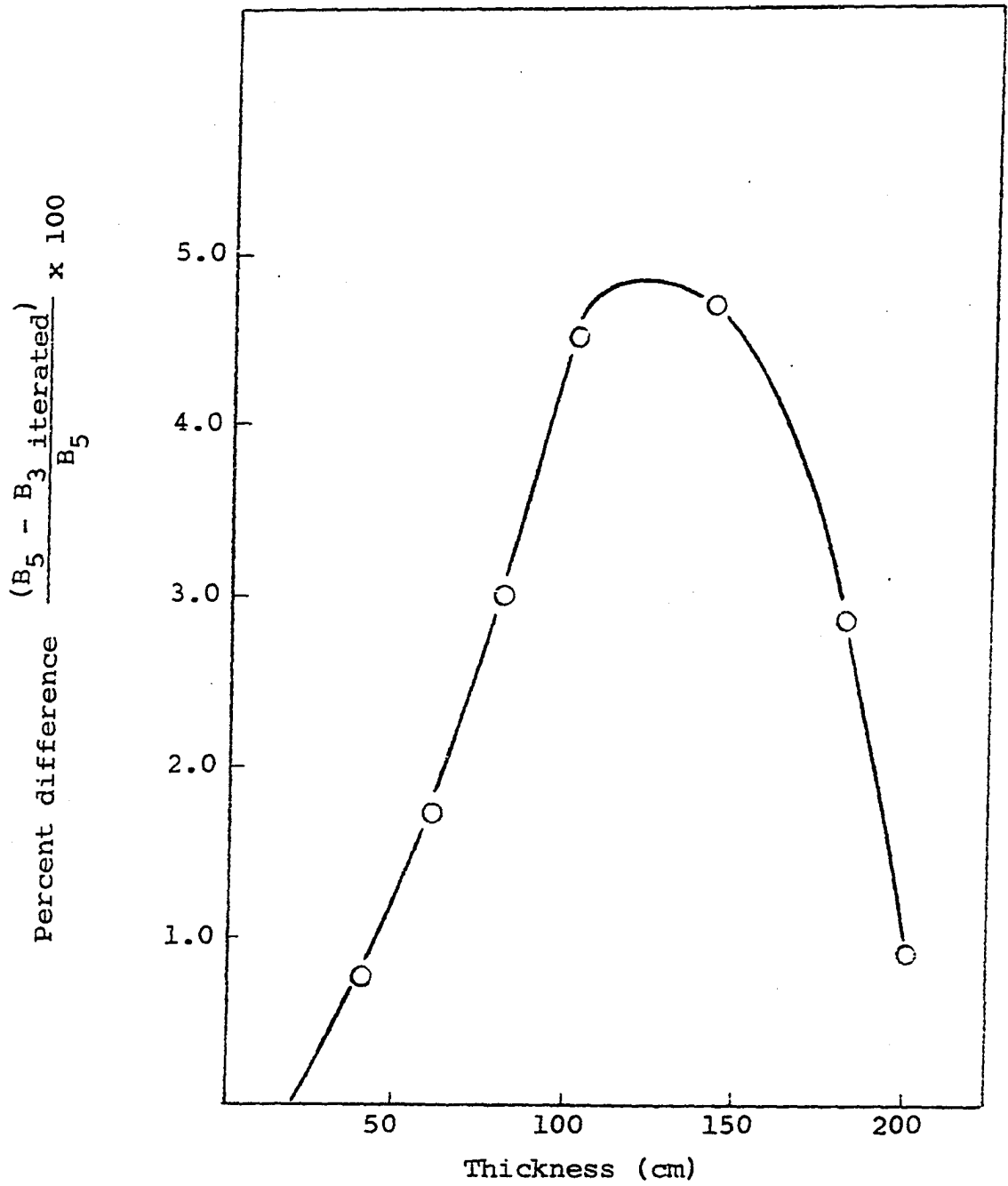


Figure 5. Percent difference in buildup factor between a five angle term non-iterated solution and a three angle term iterated solution

term buildup factors. The percentage difference between these two buildup factors is shown in Figure 5. The maximum difference is approximately five percent. Since most of the shields to be considered in the weight optimization have less than 200 cm of water, it was concluded that the three term angular expansion coupled with the iterative technique would give satisfactory results.

To pick the number of energy groups and their widths the results of Yarmush (14) and Boulette (2) are used. The results of Yarmush indicate that adequate results can be expected if energy group widths are on the order of one MeV for the energy range nine to two MeV. Boulette has shown that whenever a strong discrete energy gamma source is present the group containing this source must be narrow. As an example of this point, shown in Table 1 is a possible group structure from 9 MeV to 2 MeV where sources at 6 MeV and 3.5 MeV are present due to (n,γ) reactions with the shield materials.

Boulette has shown that below two MeV the group structure must be narrowed. This is caused by the large buildup of low energy gammas that are scattered down from the higher groups.

The energies and intensities of discrete gamma rays resulting from thermal neutron capture in iron, lead, and water (1) are shown in Table 2. The energy group structure must be chosen so that these sources of secondary gamma rays

Table 1. Example of energy group structure with secondary gamma sources

Group	Upper Energy	Lower Energy
1	9.00	8.00
2	8.00	7.00
3	7.00	6.01
4	6.01	5.99
5	5.99	5.00
6	5.00	4.00
7	4.00	3.51
8	3.51	3.00
9	3.00	2.00

may be approximated to a fairly high degree of accuracy. Individual groups for each secondary gamma ray is impossible since the resulting transmission matrix would require far too much computer storage. It was decided that the best procedure to use in picking the group structure would be to use narrow groups for the high intensity, high energy secondary gammas and wider group structure for the others. The non-narrow energy groups for the Fe - H₂O shield were chosen so that the average of the intensity times the individual secondary gamma energies in each group fell near the center of that

Table 2. Secondary gammas produced by iron, lead, and water

Fe		Pb		H ₂ O	
E MeV	I Photons/100 captures	E MeV	I Photons/100 captures	E MeV	I Photons/100 captures
10.160	0.06				
9.298	2.0				
8.872	0.3				
8.345	0.6				
7.639	29.0	7.380	93.0		
7.285	3.0				
6.369	0.3	6.734	7.0		
6.015	6.0				
5.914	6.0				
5.510	0.6				
4.968	0.6				
4.810	1.0				
4.440	1.0				
4.210	2.0				
3.860	0.7				
3.430	2.0				
3.725	1.1				
3.552	1.4				
3.430	3.9				
3.240	2.9				
3.146	2.1				
2.837	2.1				
2.730	2.9				
2.672	1.0				
2.143	1.4			2.230	100.0
1.802	2.3				
1.720	6.4				
1.626	6.1				
1.530	1.9				
1.236	1.5				
0.454	4.1				
0.364	6.7				
0.313	3.2				

Table 3. Energy group structure

Fe - H ₂ O		Pb - H ₂ O	
Group	Energy MeV	Group	Energy MeV
1	7.640 - 7.638	1	7.381 - 7.379
2	7.638 - 6.025	2	7.379 - 6.735
3	6.025 - 5.900	3	6.735 - 6.733
4	5.900 - 4.850	4	6.733 - 5.500
5	4.850 - 3.850	5	5.500 - 4.250
6	3.850 - 3.000	6	4.250 - 3.000
7	3.000 - 2.235	7	3.000 - 2.235
8	2.235 - 2.225	8	2.235 - 2.225
9	2.225 - 1.800	9	2.225 - 1.800
10	1.800 - 1.350	10	1.800 - 1.350
11	1.350 - 0.900	11	1.350 - 0.900
12	0.900 - 0.400	12	0.900 - 0.400
13	0.400 - 0.100	13	0.400 - 0.100

group. It was felt that this approach would minimize any error caused by not using narrow groups for all the secondary gamma energies. Table 3 presents the group structures used for the iron-water shields and the lead-water shields.

Before the weight optimization procedures were carried

out it was desirable to verify Equation 25, and the computer program that was written which uses it to calculate dose. Comparison was made between the terms in Equation 25 and the published shield calculations for the N. S. Savannah reactor (11). The primary shield for the Savannah reactor is shown in Figures 6 and 7. The shield consists of laminae of steel and water, the steel being the shaded areas in Figures 6 and 7. Using Equation 25 the fast neutron flux, thermal neutron flux, and secondary gamma dose were calculated for this shield configuration. These results are shown on Figures 6 and 7 along with the results of the calculations carried out by Smith and Turner (11).

In Figure 6 one notes the agreement between the fast flux as calculated using Equation 25 and the results from Smith and Turner is quite good. The thermal fluxes agree early in the shield and then some deviation is noted. This disagreement is probably caused by convergence difficulties in the two group computer program used to calculate the thermal flux in Equation 25. This disagreement deep into the shield is not important because the thermal flux in the water contributes very little to the total secondary gamma dose which is observed at the outside of the shield.

In Figure 7 one can note that the secondary gamma dose calculated using Equation 25 is consistently lower than the values given by Turner and Smith. The doses shown by Turner

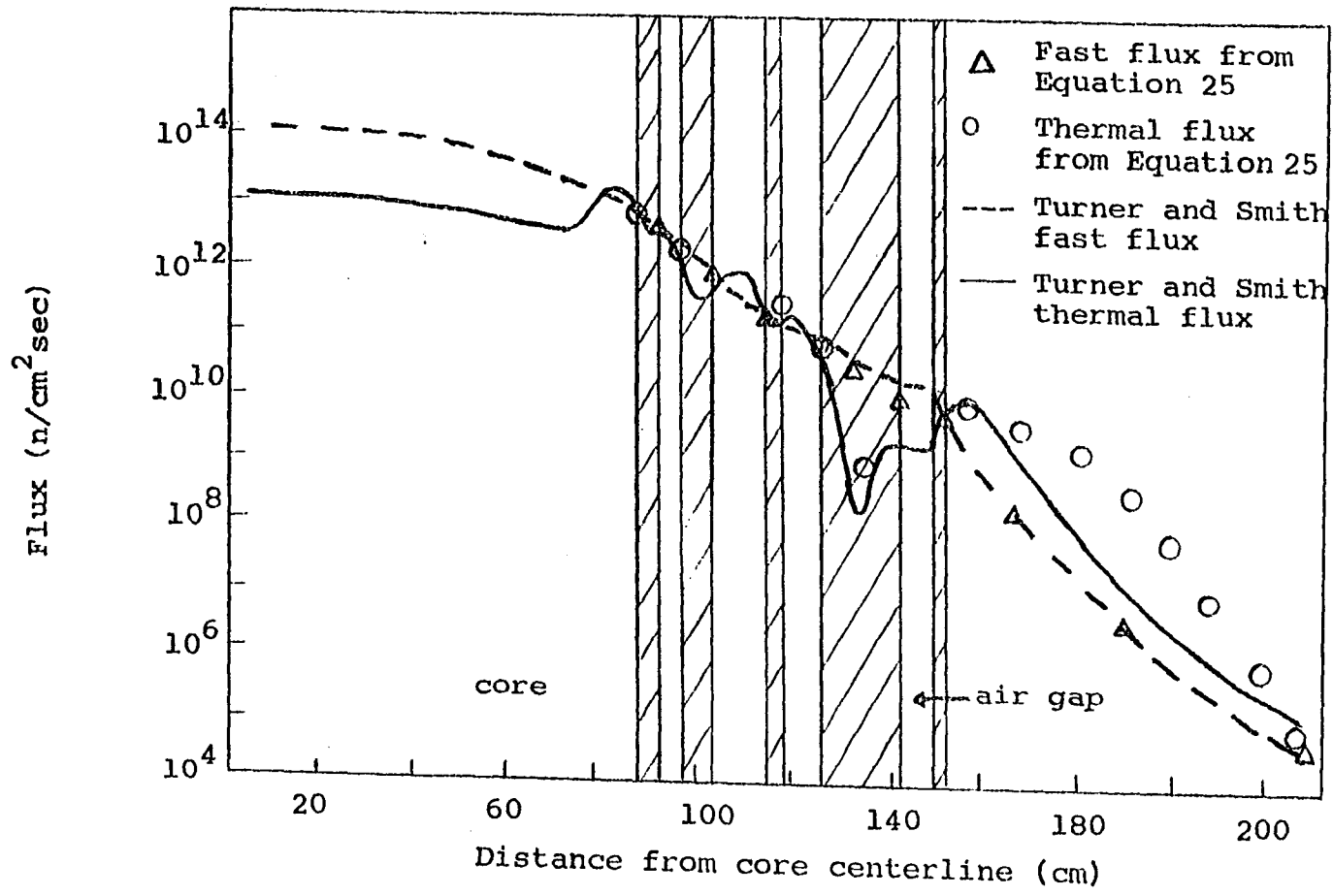


Figure 6. Comparison of neutron fluxes

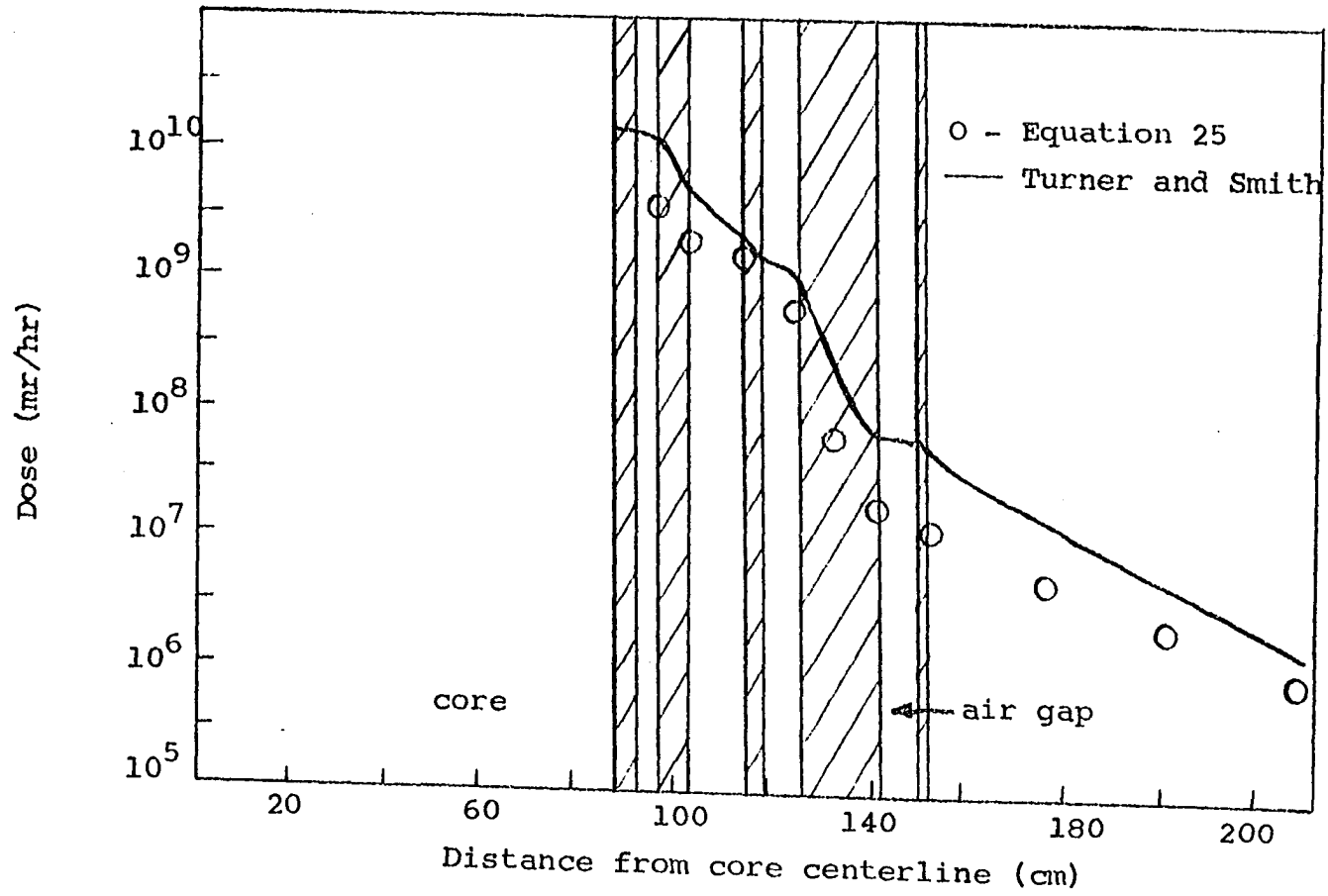


Figure 7. Comparison of secondary gamma dose

and Smith are those which would be obtained if a detector were placed in the shield, that is, the total secondary gamma dose as a function of position in the shield. This is obtained by adding the contributions from all the secondaries produced both to the right and the left of the point in question. The secondary gamma dose as calculated by Equation 25 is not the total dose. Equation 25 yields what is best described as a secondary gamma current dose. This is the dose that would be observed if the shield were terminated at that point. Equation 25 does not consider secondary gamma rays produced to the right of the point in question. One cannot convert the results of Equation 25 to those of Turner and Smith by a simple multiplicative factor since the amount of feed back will vary with location.

Another possible cause of the difference between the two sets of results was the slab thicknesses. Transmission matrices were used only for two cm of Fe and three and nine cm of water. It was thus necessary to approximate the Savannah shield with laminae of these thicknesses. This approximation would cause some additional differences between the two results.

It was impossible to compare results on primary gamma transport through the Savannah shield because of lack of data. It was necessary to know the exact input quantities in terms of total input energy in each group, which was not

available.

This comparison between the terms (used to calculate fast neutron flux, thermal neutron flux, and secondary gamma dose) in Equation 25 and the data given by Smith and Turner leads to the conclusion that Equation 25 is accurate enough to be used in calculating reduced weight shields. The observed differences between the two sets of results are either of little importance to the total dose observed at the outside of the shield, or can be explained in terms of differences in the types of data presented.

Input Parameters

In order to make the optimization results as meaningful as possible data from an actual reactor was used for inputs of radiation to the shield. The New Production Reactor (N-Reactor, Hanford Atomic Products Operation, Richland, Washington) data were used (4). The reactor core is a rectangular graphite cube 23 x 24 x 35 ft. Surrounding the core is a 120 cm graphite reflector followed by concrete shielding. Data at the inside of the shield from the reactor while operating at 100 MW thermal power is as follows:

Fast Neutron Flux = 3×10^6 n/cm²sec

Thermal Neutron Flux - 1.5×10^{10} n/cm²sec

Gamma Dose - 5×10^7 mrem/hr.

The values given for the fast and thermal flux were used as boundary conditions in Equation 23 and 24 which were used to determine the thermal flux distribution in the various shield configurations that were considered in the weight optimization. $\Phi_f(0)$ in Equation 25 was set equal to the above fast flux.

$\bar{\phi}_1$ was determined such that the input primary gamma dose was 5×10^7 mrem/hr. Results stated by Blizard (1) show that the source spectrum for all gamma rays resulting from one fission in U^{235} is

$$N(E) = 14.0 \exp[-1.10 E] \quad \text{fission}^{-1} . \quad (26)$$

Integration of Equation 26 over the energy groups given in Table 3 yields the source strength of each group per fission per cm^3 per second

$$S_{v,g} = \int_{E_g}^{E_{g+1}} 14.0 \exp[-1.10E] dE \quad \text{MeV/fission cm}^3 \text{sec} . \quad (27)$$

This volumetric source was then transformed into an isotropic surface source (3).

$$S_{a,g} = \frac{S_{v,g}}{2\bar{\mu}_g} \quad \text{MeV/fission cm}^2 \text{sec} , \quad (28)$$

where

$\bar{\mu}_g$ = average attenuation coefficient for the energy group of the materials in the core.

The dose into the shield per fission was then calculated

$$D = \sum_{i=1}^{13} D_i S_{a,i} \quad \text{mrem/hr fission}$$

where

D_i = conversion factor for each group from $\text{MeV/cm}^2\text{sec}$
to mrem/hr .

Finally the individual group values of $\bar{\phi}_1$ were calculated by scaling this dose to 5×10^7 mrem/hr

$$\bar{\phi}_{1,g} = \frac{5 \times 10^7}{D} S_{a,g} \quad \text{MeV/sec cm}^2 \quad . \quad (29)$$

The total input primary gamma dose is now equal to the desired 5×10^7 mrem/hr .

Weight Optimization

As stated in the introduction, the early work on weight optimization involved calculus of variation techniques. In using this technique researchers were forced to simplify the equations which describe the transport of the radiation through the shield. These simplifications were necessary to reduce the equations to a form which could be solved by formal variational techniques. As a result of these simplifications, the accuracy of the results presented by these researchers is questionable. Mynatt (7, 8) attacked the

problem with the opposite point of view. In his work the transport of the radiation was calculated to a high degree of accuracy and simplifications were made on the optimization procedure. The optimization procedure involved calculating the weight of numerous shield configurations which reduce the output dose to the same level. Using these data the derivative of dose with respect to weight was calculated and the configuration which reduces this derivative to zero was taken as the optimum. They discovered that this procedure works well for shields that are relatively simple, but as the number of laminae are increased difficulties arise in calculating the needed derivatives.

In this investigation a procedure similar to that used by Mynatt (7, 8) was employed. The weight of numerous shield configurations which reduce the output dose to some constant value was calculated using Equation 25. The weight as a function of some configuration parameter was then plotted and a minimum was sought.

RESULTS

In Figures 8-15 the results of the weight optimizations are presented. The figures are used to determine the best location of the heavy material, lead or iron, in the water. Results also show the proper thickness of the heavy material and the effect on the weight of the shield when this thickness is divided into a number of slabs separated by slabs of water. For a fast reactor the variation of shield weight as a slab of heavy material is moved away from the reactor core is determined. Finally, data are presented which show the effect on shield weight when the input parameters are varied. Except for the fast reactor results all the figures are based on the input parameters chosen in the previous section.

Slab Shields

The total weight of the shield as a function of thickness of heavy material is shown in Figure 8. In this figure the heavy material is placed against the reflector and is followed by water. Results for both lead and iron are presented. The input dose is 1.07×10^8 mrem/hr. The desired dose at the outside of the shield was set at 10^4 and 10^5 mrem/hr so that comparison between the curves for different cutoff doses could be made. Several important points can be

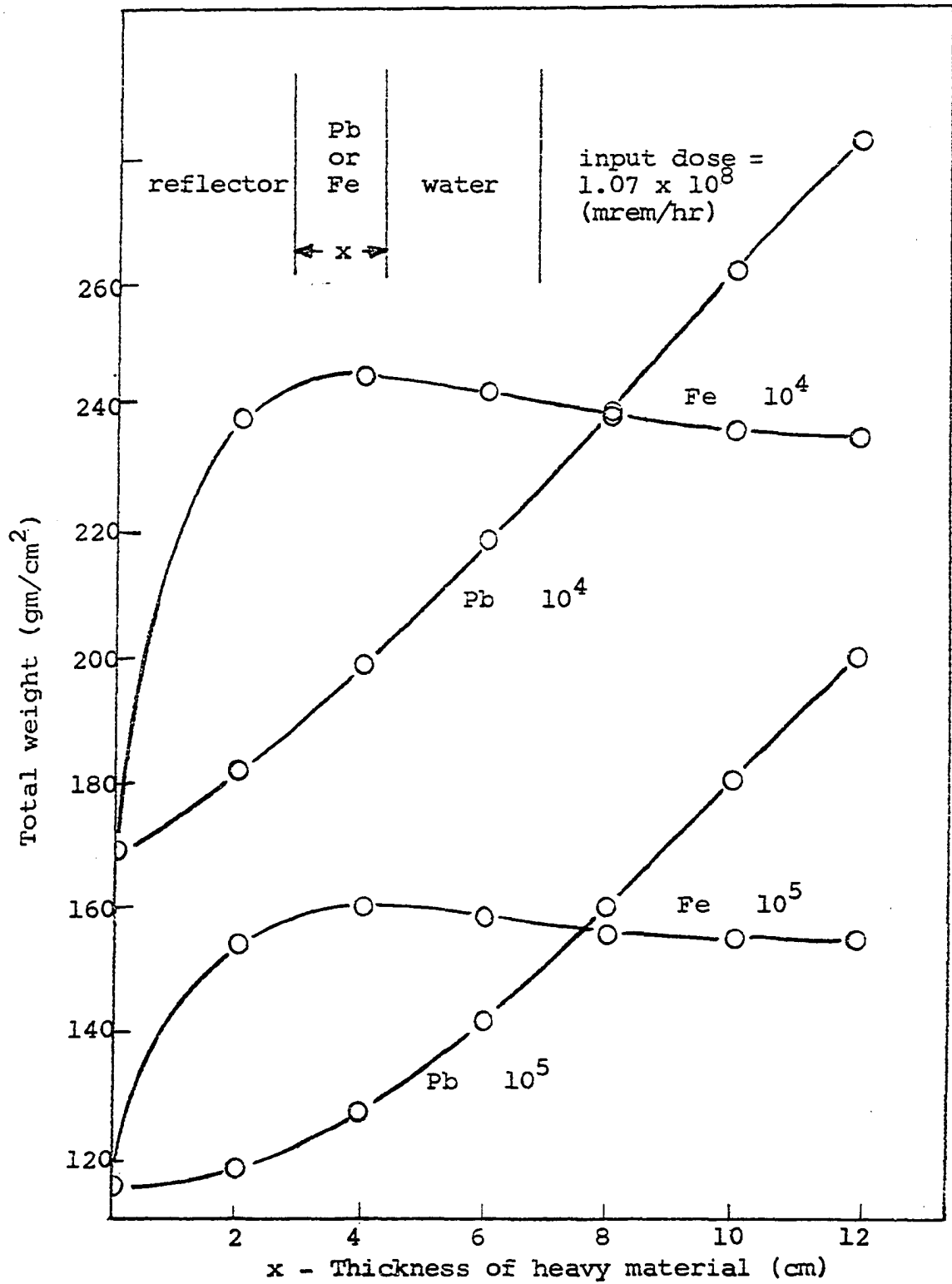


Figure 8. Total weight versus heavy material thickness

noted from these curves. For both cutoff doses and both heavy materials one can note that the lightest shield is the one in which no heavy material is present, i.e. all water. In other words, no weight reduction is obtained by placing heavy material next to the reflector. The observed increase in weight is caused by the large number of high energy secondary gammas which are produced in the heavy material.

One also can notice that for thin slabs of lead produces a lighter shield than iron, but beyond eight cm of lead the opposite is true. This effect is caused by differences in the capture cross section of the two materials. The capture cross section of iron is more than thirty times that of lead. Due to this difference in cross section, the thermal neutron flux profile in the lead is much flatter than in the iron. In the iron most of the secondaries are produced in the first few centimeters of the slab, while in the lead they are produced at almost an equal rate throughout the slab. This results in a much larger self shielding effect in the iron, since most of the secondaries must travel through several centimeters of this heavy material which in turn attenuates them greatly. In the lead this effect is not as dominant because the secondaries are produced equally through the slab; therefore the ones formed near the end of the slab are not attenuated by the lead. This self shielding effect is also shown in Figure 9. In this figure is shown the total

weight of the water behind the different thicknesses of heavy materials.

The shape of the curves for the different cutoff doses are seen to be similar. This comparison was carried out to determine if the shape of weight curves, such as shown in Figures 8 and 9, were a strong function of the cutoff dose. Since little or no change is noted as the cutoff dose is changed, it is concluded that no strong dependence exists between the shape of the curves and the cutoff dose. This result of course cannot be extrapolated many orders of magnitude without further verification.

From the results of Figures 8 and 9 it has been concluded that the heavy material must be moved away from the reflector in order to decrease the secondary gammas produced by thermal neutron capture. Since it is desirable to decrease the thermal neutron flux the water was borated. A saturated solution of boric acid in water was assumed in place of the previously pure water. The curves in Figure 10 show the effect of moving the heavy material slabs away from the reflector. Data is shown for heavy material slab thicknesses of eight cm of Fe, six and eight cm of Pb. The rapid decrease in weight as the thickness of the leading borated water slab is increased is due to the decrease in the number of secondaries produced in the heavy materials. This is of course the result of lowering the thermal flux in these

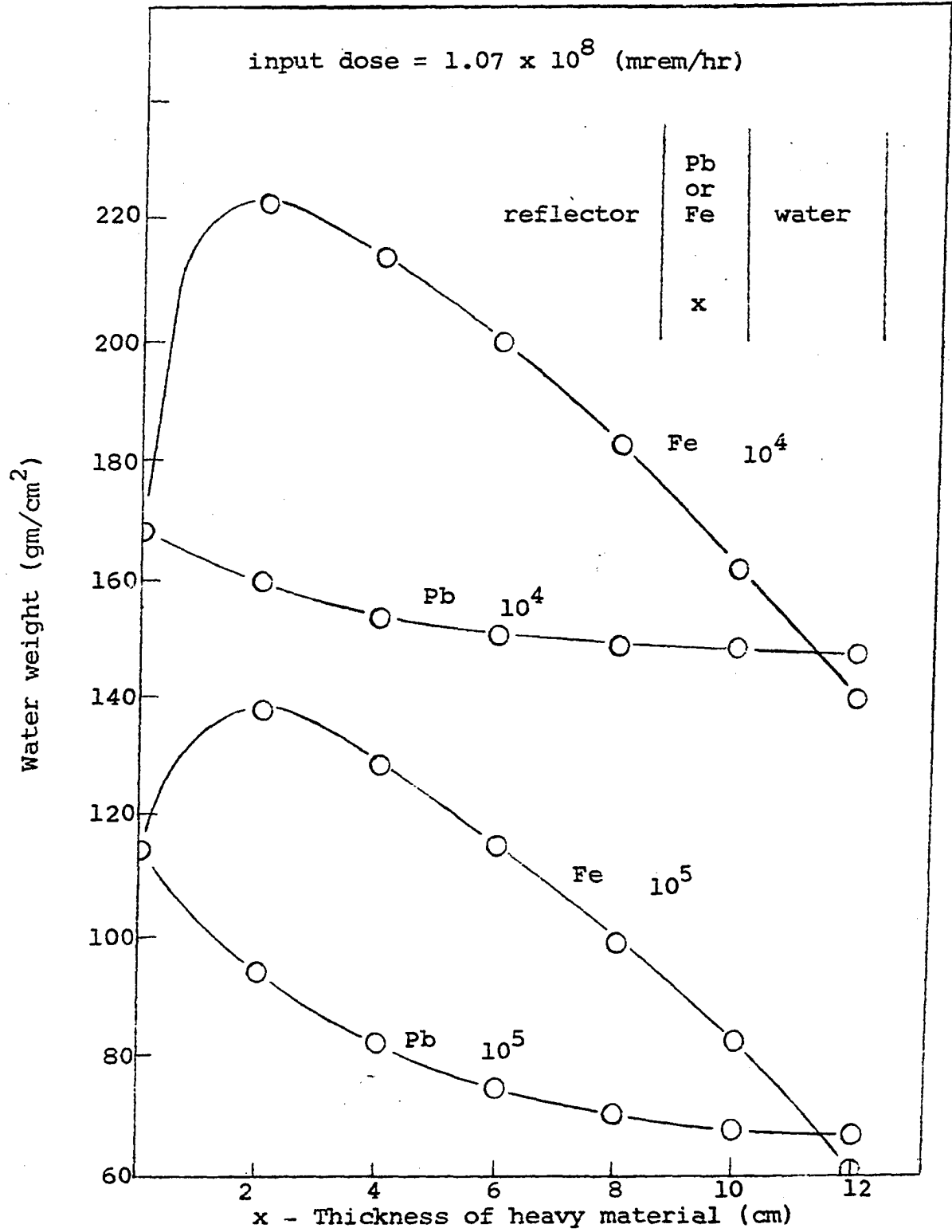


Figure 9. Water weight versus heavy material thickness

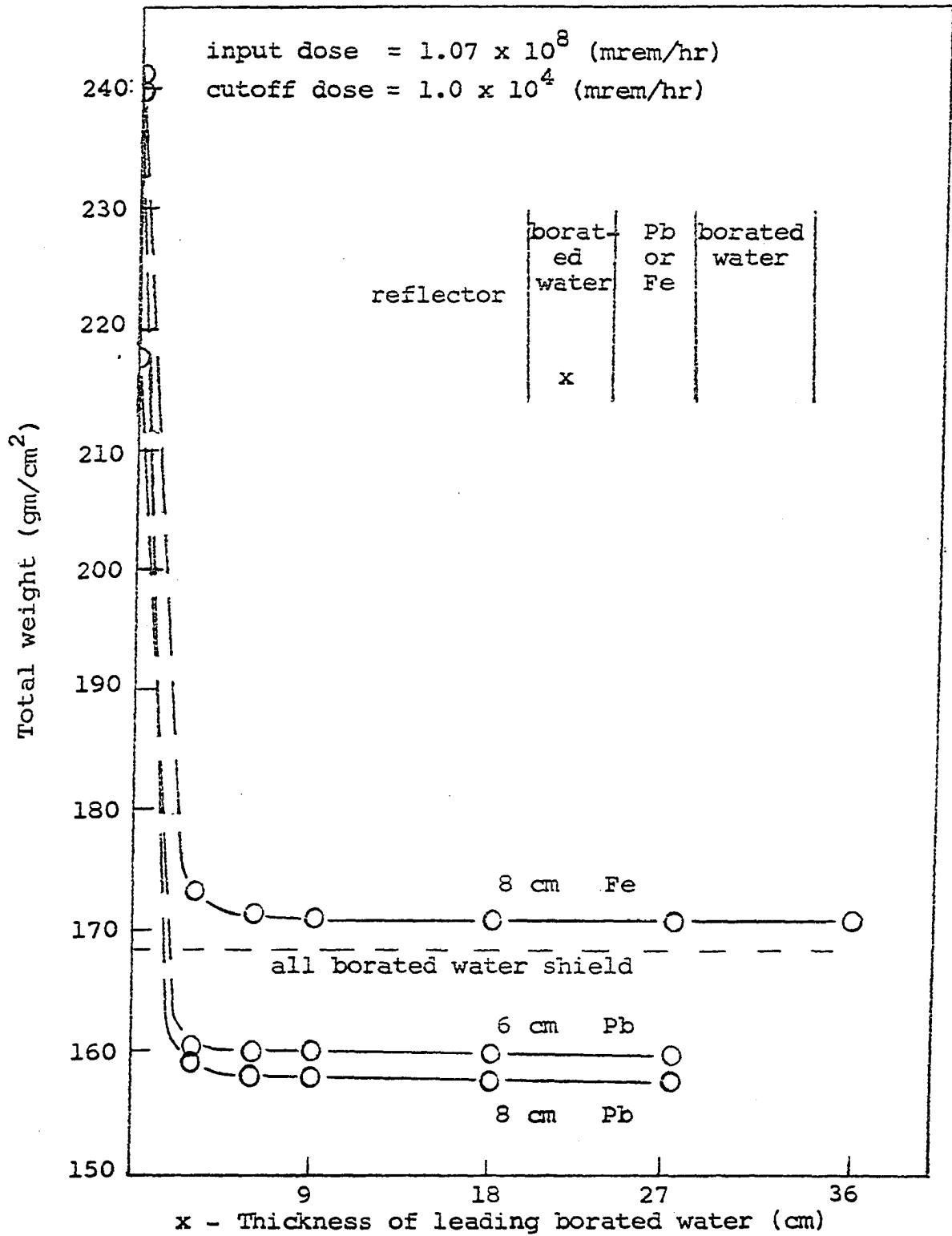


Figure 10. Total weight versus position of heavy material

heavy materials.

One can note that this rapid decrease in weight as the lead slab is moved away soon ends and the total weight becomes nearly independent of the location of the heavy slab. This effect is caused by the primary gamma rays. With the heavy material more than about six cm into the borated water, the secondary gammas cease to be significant to the total dose at the outside of the shield. The dose at the outside edge of the shield is essentially due to primary gammas. Therefore the weight of the shield ceases to be a function of the location of the heavy slab because the attenuation of the primary gammas is not dependent on the location of the heavy material. In actuality some slight dependence does exist between the attenuation of the primary gammas and the location of the heavy slab since slight changes in the buildup effect will result as the slab is moved.

One can notice from Figure 10 that the weight of the shield containing eight cm of iron becomes insensitive to the heavy slab location at a higher value than an all water shield. This result is expected since the mass attenuation coefficient (cm^2/gm) of iron is less than that of water. In other words, on a per unit weight basis iron is a poorer gamma shield than is water. Lead, however, is a better gamma shield per unit weight than water and a shield containing lead is expected to become insensitive at a lower weight

than an all water shield. This is shown on Figure 10 for the shields containing six and eight cm of lead.

It has been determined that a reduced weight shield can be constructed by placing a lead slab behind at least six cm of borated water, the lead slab to be followed by more borated water. It remains to determine the optimum thickness of this lead slab. It also remains to determine if splitting the lead slab into several thinner slabs, separated by borated water, produces any further weight reduction. Figure 11 is used to determine the optimum lead thickness. Plotted in the figure is the total shield weight as a function of the lead slab thickness. The lead slab is separated from the reflector by nine cm of borated water. The weight first decreases, goes through a minimum, and then increases. The weight decrease, as the lead thickness is increased, is caused by the increased capacity of the shield per unit weight to attenuate primary gammas. The final increase in the weight is caused by fast neutrons. As the lead slab thickness is increased less and less water is required to attenuate the primary gammas and the water thickness is thus decreased. The water, however, also served to reduce the fast neutron flux. The contribution to the total dose from the fast neutrons increases as the water thickness is decreased and eventually becomes an important factor. It is this increased fast neutron dose which causes the shield

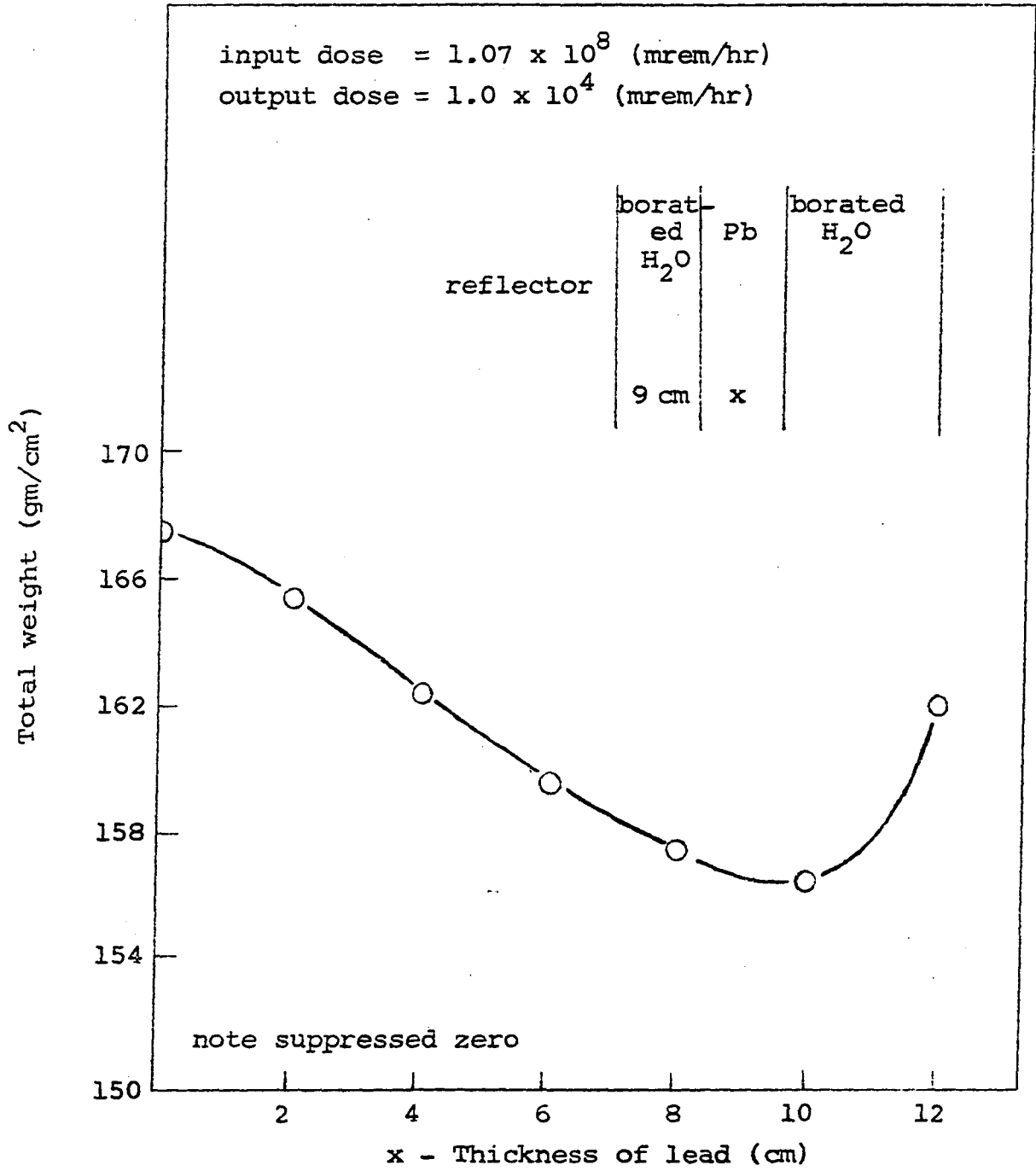


Figure 11. Total weight versus lead thickness in borated water

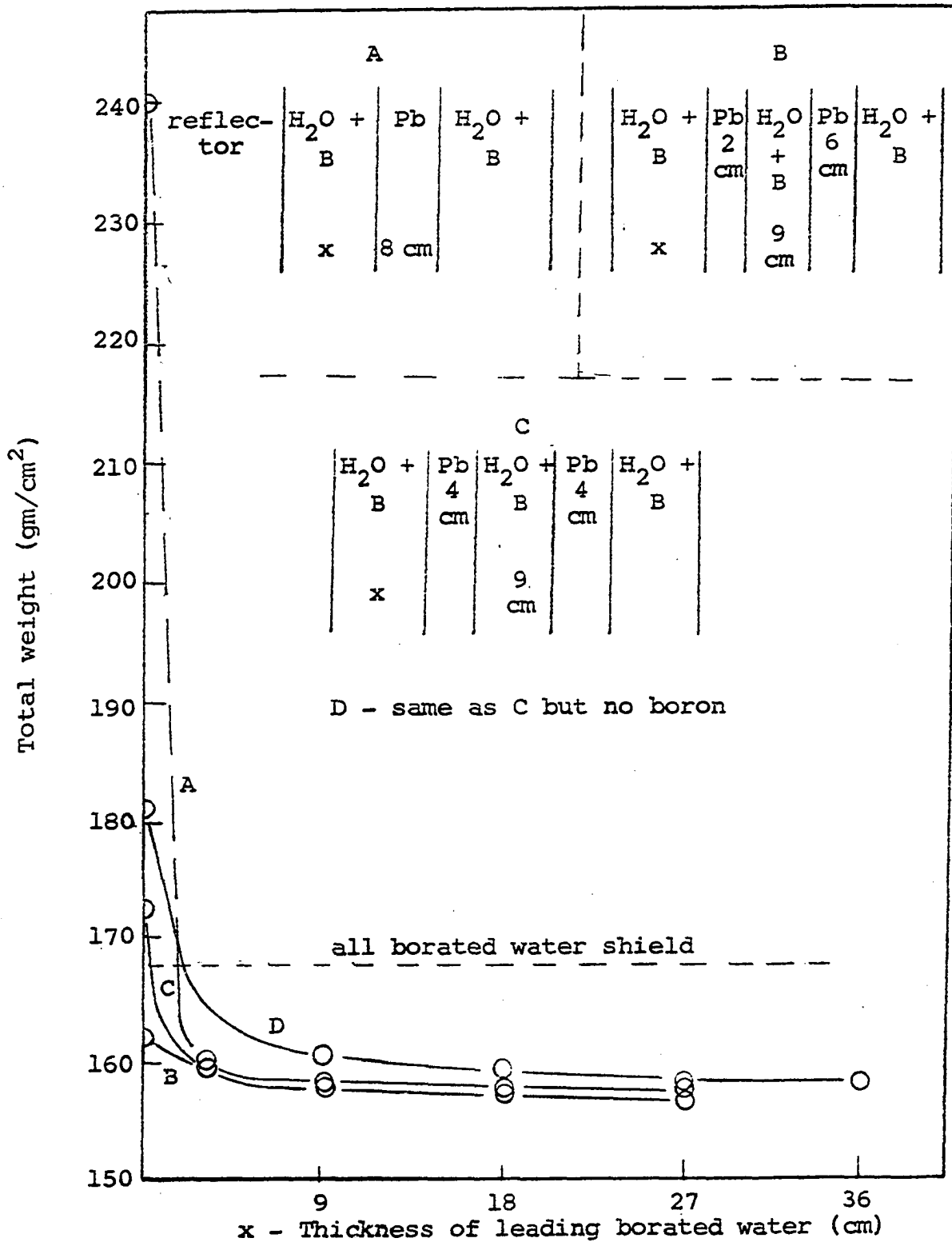


Figure 12. Effect of lamination on shield weight

weight to increase in the latter portion of Figure 11.

The results of the study used to determine if further weight reduction is possible through the lamination of the lead slab are shown in Figure 12. If separated from the reflector by a few centimeters of borated water, the results show that little or no further weight reduction is obtained by lamination of the lead slab. Significant weight reductions are possible if part of the lead slab is constrained to be next to the reflector.

One can conclude from the results presented thus far that the optimum design to produce a minimum weight shield is approximately 9 cm of borated water, followed by 9.5 cm of lead, in turn followed by 40 cm of borated water. No appreciable weight reduction is accomplished by splitting up the 9.5 cm slab of lead. This configuration leads to a 6.5 percent reduction in total shield weight over that obtained for a pure water shield.

Cylindrical Shields

The results presented thus far are for infinite plane slab shields. Actual reactors are generally cylindrical in shape and therefore the shielding is also cylindrical. Weight curves, similar to Figure 10, were obtained by using an approximate conversion for dose from an infinite slab to dose from an infinite cylinder (3)

$$D_{cy}(r_o) = \sqrt{\frac{r}{r_o}} D_{PL}(r_o) \quad , \quad (30)$$

where

$D_{cy}(r_o)$ = dose at a distance r_o from the axis of an infinite cylinder

$D_{PL}(r_o)$ = dose at distance (r_o-r) from an infinite plane located at (r_o-r)

r = radius of the infinite cylinder.

A core plus reflector radius of 200 cm was assumed, i.e. $r = 200$ cm, and the input parameters were assumed the same as for the slab case. The total weight of this cylindrical shield as a function of the location of the heavy material annuli is shown in Figure 13. Comparison of Figures 10 and 13 show that for cylindrical geometry the Fe - H₂O shield is lighter than the all H₂O shield, while the opposite is true for slab geometry. In both cases the Fe - H₂O shield is much thinner than the all H₂O shield, but cylindrical geometry, or spherical, is required to show the importance of this in terms of weight reduction. This result is due to the shield weight increasing as the square of the shield thickness for cylindrical geometry. Cylindrical geometry also increases the percent weight reduction of the optimum shield over an all water shield. When transformed to cylindrical geometry the optimum configuration, for the slab geometry, produces a 30 percent weight reduction.

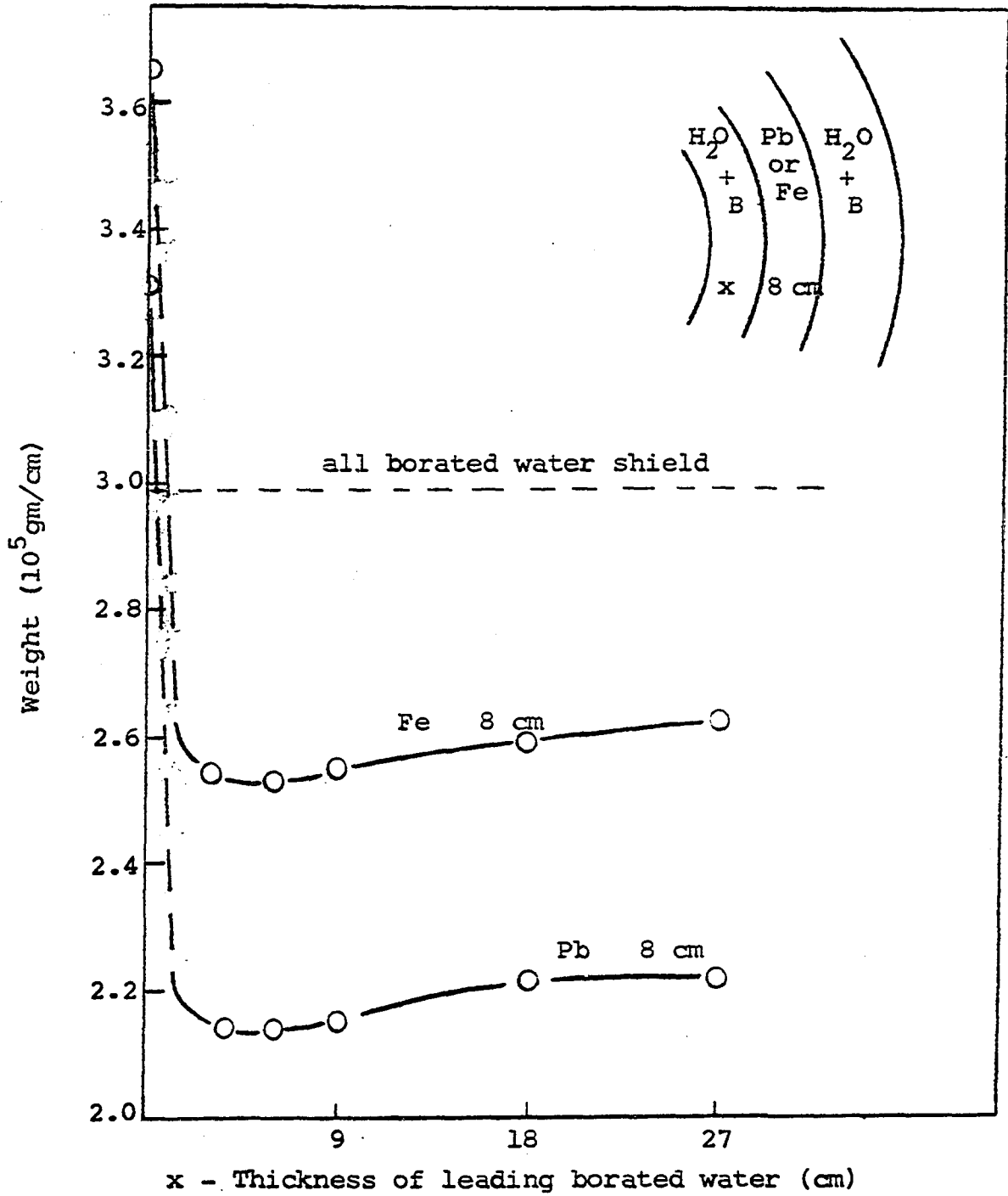


Figure 13. Total weight versus heavy material location for a cylindrical reactor

Fast Reactor Shields

The input parameters to a fast reactor shield are greatly different from those for a thermal reactor shield. The minimum weight shield configuration for a fast reactor is thus expected to be different from a thermal reactor.

The total weight of a fast reactor shield as a function of the leading borated water thickness is shown in Figure 14. Input parameters for this shield were determined by assuming various reactor parameters and calculating the desired quantities. The following assumptions were made:

$$\text{core power} = 2500 \text{ MW}_T$$

$$\text{core volume} = 2400 \text{ L} = 2.400 \times 10^6 \text{ cm}^3$$

$$\text{volume percents} = 40\% \text{ Na}$$

$$10\% \text{ AL}$$

$$50\% \text{ Fuel}$$

$$\text{Enrichment} = 20\% \text{ U}^{235}.$$

Using these values in Equation 31 the average fast flux was calculated

$$\phi_f = \frac{2.500 \times 10^9 \text{ watts} \times 3.1 \times 10^{10} \text{ watts/fission}}{\text{Volume } \Sigma_f}, \quad (31)$$

$$= 4.83 \times 10^{15} \text{ n/cm}^3 \text{ sec}$$

where Σ_f is the macroscopic fission cross section and was obtained from a one group fast reactor cross section table (13).

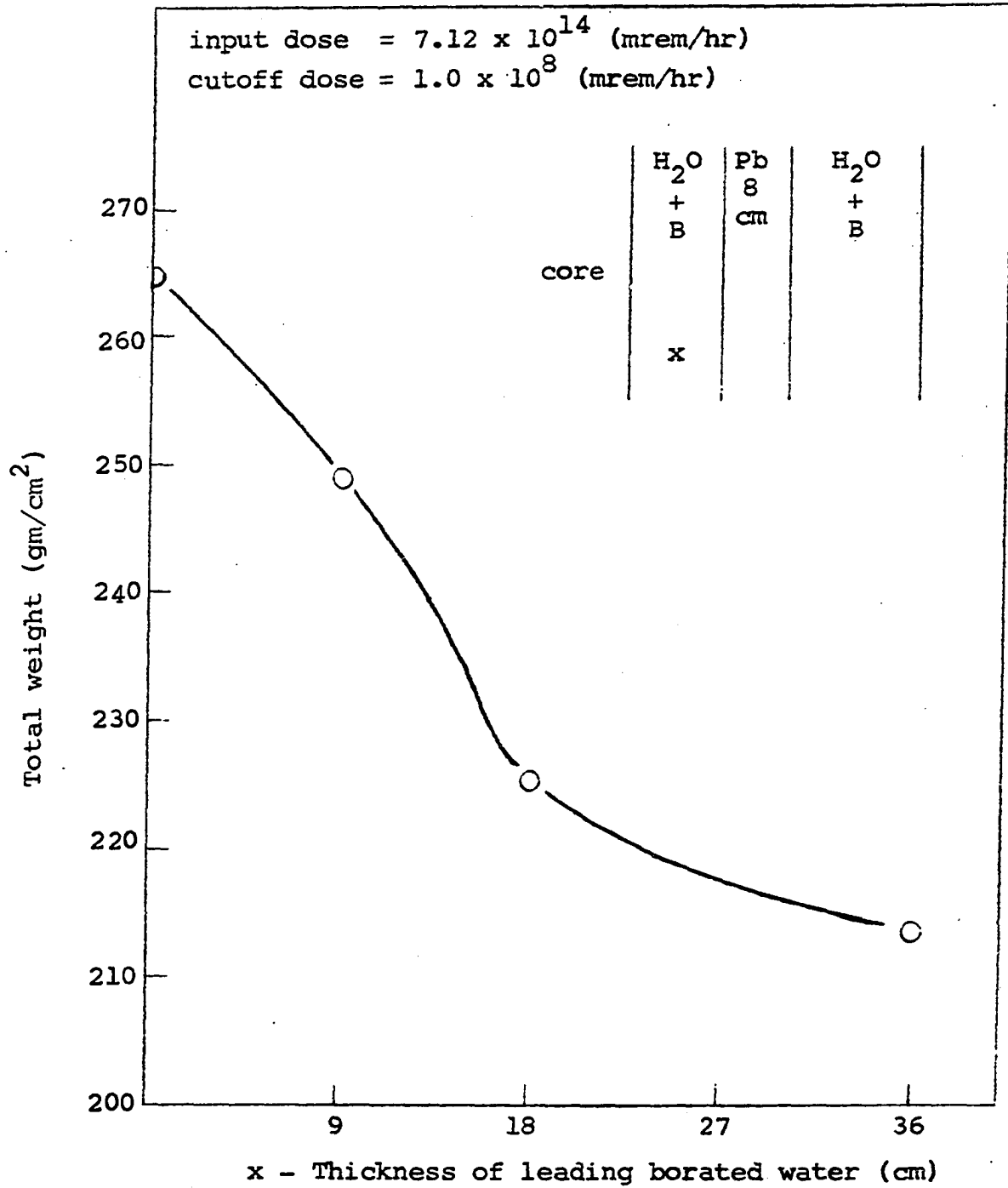


Figure 14. Total weight versus heavy material location for a fast reactor

This average value for the fast flux was assumed as an input to the shield. The input primary gamma spectrum was obtained by multiplying the isotropic surface sources, as given by Equation 28, times the fission rate. This yields a total input gamma dose of 9.66×10^{11} mrem/hr. It is interesting to note that for the fast reactor the total input dose is almost entirely due to fast neutrons, while for the thermal reactor the predominant factors were the primary gammas and the thermal neutrons.

One can note from Figure 14 the weight does not decrease as rapidly as it did in Figure 10 for the thermal reactor. Thermal neutrons being fed down from the fast flux continue to produce large numbers of secondary gammas as the leading water thickness is increased. Eventually the fast flux, and resulting thermal flux, decrease to a point where they become unimportant and the curve begins to approach a nearly constant value as it did for the thermal reactor. The important point to note is that a much larger leading thickness of borated water is required in a fast reactor if one wishes to minimize secondary gamma ray production.

Input Parameter Variation

A study was conducted to determine what changes in total shield weight could be expected if the input parameters (primary gamma dose and thermal neutron flux) were changed. This

information is useful in understanding which parameters are controlling the shield weight. It is also useful in determining reduced weight shields for reactors with slightly different input parameters from those used in this investigation.

The results of this study are shown in Figure 15. The shield is eight cm of lead surrounded by 80 cm of borated water. The abscissa is the thickness of borated water between the reflector and the lead. The ordinate is the ratio of the dose which penetrates this shield for the changed input parameters, to the dose which penetrates it for the original input values. Two different perturbations were studied. The input thermal flux was increased by factors of 2, 5, 10, and 100 over the NPR value. Identical perturbations in the input primary gamma dose were carried out. The curves which decrease as the leading water thickness is increased pertain to the neutron perturbations while those that increase pertain to the gamma perturbations. Two important points should be noted from the curve. Little change in the output dose is observed when the thermal neutron flux is changed, if the lead slab is preceded by about 12 cm of borated water. On the other hand, for leading slabs thicker than about 6 cm of borated water a change in the input primary gamma dose causes an almost equal change in the output dose.

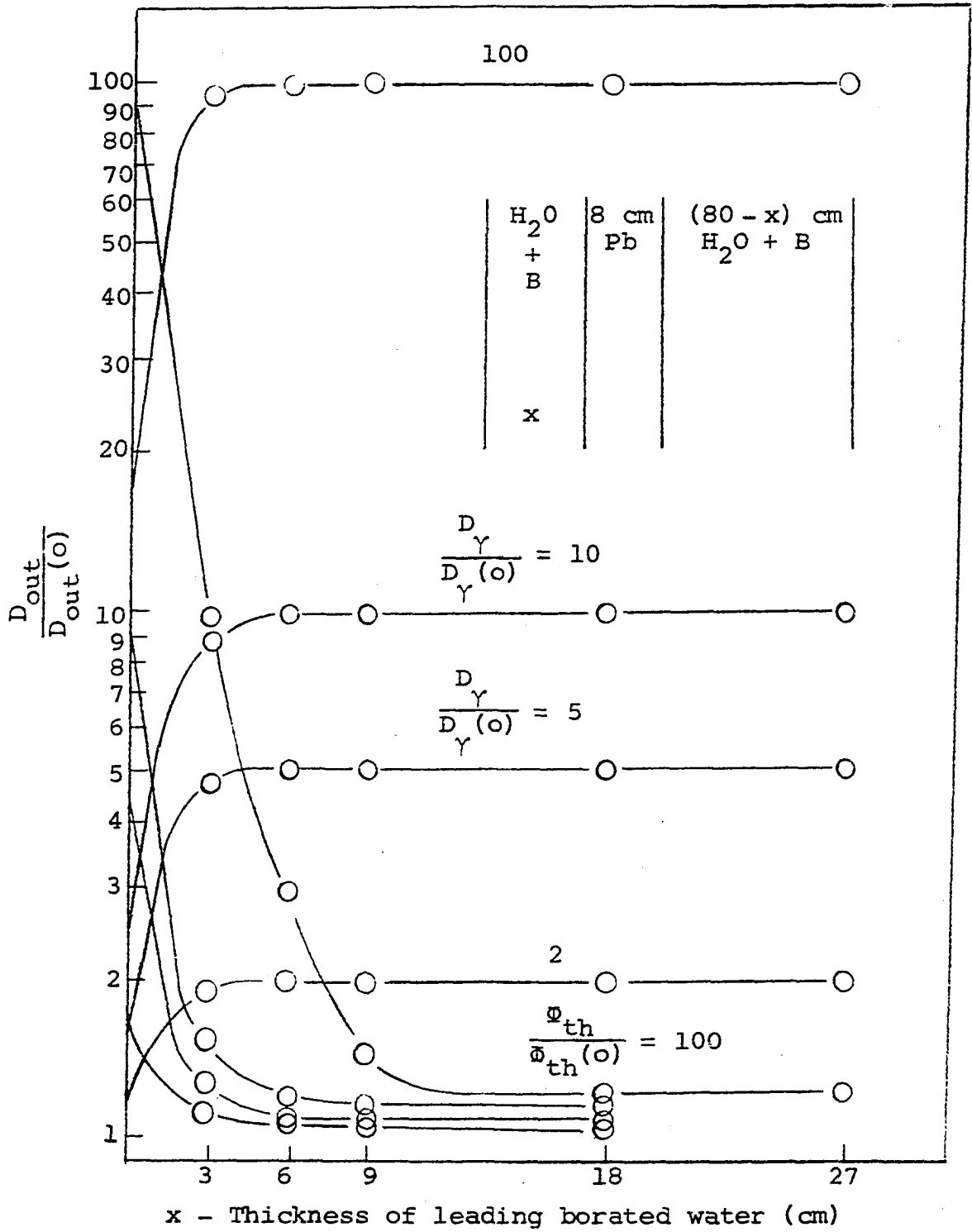


Figure 15. Dose changes versus location of lead slab

SUMMARY OF RESULTS

This investigation had two basic purposes. The first was to develop a quick and accurate method of calculating dose rates outside the primary shield of a nuclear reactor. The second purpose was to use this method to investigate minimum weight reactor shield configurations. The contribution by this investigator was the adaptation of the transmission matrix method to an actual shield design problem and then using this method to obtain reduced weight primary shields.

Results show that the transmission matrix method can be used for primary and secondary gamma rays to obtain dose rates outside a laminated reactor shield. A three term Legendre polynomial expansion for the angular dependence of the gamma rays was found to be sufficient for purposes intended. It was discovered that the individual homogeneous slabs of shielding materials could be considered to be composed of thinner lamina of the same material. Thus it was not necessary to calculate transmission matrices for the total shield investigated in the weight optimization. The concept of using narrow energy groups for intense high energy secondary gamma sources and wider groups where these sources were not present, was found to be satisfactory.

The weight optimization study for the laminated thermal

reactor slab shield lead to several important results. The distance from the reflector to the heavy material was found to be the most important factor in designing a minimum weight shield constructed of water and lead or iron. Placing the heavy material directly against the reflector caused a weight increase over an all water shield. This is due to large numbers of secondary gammas formed in the heavy material by the high thermal neutron flux observed at this location. Borating the water and moving the lead slab away from the reflector resulted in a reduced weight shield. The minimum weight configuration was found to be 9 cm of borated water, followed by 9.5 cm of lead, in turn followed by 40 cm of borated water. This configuration lead to a 6.5 percent reduction in total shield weight over that obtained for an all water shield. No further appreciable weight reduction was obtained by dividing the lead slab into several thinner slabs. Weight reductions of over 40 percent between shields where the heavy material is directly behind the reflector, and the minimum weight configuration were observed.

As a slab of lead was moved away from the reflector the radiation which caused the largest portion of the dose at the outside of the shield changed. Secondary gamma rays caused the largest portion of the dose when the lead slab was close to the reflector. At larger distances primary gammas were the predominant factor. Fast neutrons became

the most important factor when the lead thickness exceeded about 10 cm.

The minimum weight configuration for a cylindrical reactor shield yielded a weight reduction of 30 percent. The larger reduction, when compared to the slab shield value of 6.5 percent, was due to the radius squared weighting that exists for cylindrical geometry. Slightly larger reductions would be expected for spherical geometry.

The results for a fast reactor indicate that the thickness of the borated water slab between the core and the lead slab must be larger than for a thermal reactor. This is caused by the high thermal neutron flux which exists deep into the fast reactor shield. This thermal flux is produced by the slowing down of the fast neutrons in the shield.

Perturbation of the input thermal neutron flux for the thermal reactor produced no appreciable change in the output dose for a shield configuration near the optimum. For non-optimum shield configurations large changes in output dose were observed. Increases in the input gamma dose produced an almost equal change in the output gamma dose for shield configurations near the optimum. At non-optimum configurations little change is observed because the output dose was mostly due to secondary gammas.

SUGGESTIONS FOR FURTHER STUDY

In this investigation the transmission matrix method was used only for the primary and secondary gamma rays. It would be desirable in future investigations to employ this method for neutron transport in the reactor shield as well as the gamma rays. Use of the transmission matrix method would replace the two group diffusion approximation used in this investigation by a multigroup solution to the transport equation. This would result in a higher degree of accuracy for the neutron transport. It might also be possible using this technique to incorporate secondary gammas produced by inelastic scattering of fast neutrons. It should be noted that major difficulties might develop with this method of solution for the neutron transport since the iterative technique used in this investigation could not be used. One possible solution to this problem involves the use of doubling techniques as discussed by Pfeiffer (9).

The energy group structure used for the gamma rays is another area which needs to be investigated further. Optimum group structures for different materials need to be determined. This optimization would involve determining the number, location, and width of the energy groups for various materials and material combinations. It would be ideal if one group structure could be obtained that would be satis-

factory for most common reactor shielding materials.

Techniques need to be developed which will enable the transmission matrix method to solve accurately deep penetrations (greater than 200 cm of water) into the shield. This would involve the use of higher order Legendre polynomial expansions for the angular dependence of the flux. It is possible that techniques could be developed where high order expansions are used for energy groups where large amounts of forward peaking develop, and lower order expansions for groups where this peaking does not become important. Such a technique would enable one to investigate the weight optimization of the total reactor shield instead of just the primary shield.

Finally optimization of other parameters could be investigated. Minimum volume primary shields would be of use under certain circumstances. Cost minimization where construction difficulties are considered is another possibility. Optimization where constraints are imposed could also be considered. Such a constraint might be some required minimum thickness of the pressure vessel of the reactor which is usually considered part of the primary shield. Optimization to minimize heating in the primary shield is also of interest.

LITERATURE CITED

1. Blizard, E. P. and Abbot, L. S. Reactor handbook. Volume III, Part B: Shielding. 2nd ed. New York, N.Y., Interstate Publishers. 1962.
2. Boulette, E. T. Applications of the transmission matrix method to neutron and gamma transport. Unpublished Ph.D. thesis. Ames, Iowa, Library, Iowa State University of Science and Technology. 1968.
3. Glasstone, S. and Sesonske, A. Nuclear reactor engineering. New York, N.Y., D. Van Nostrand Company, Inc. 1963.
4. Greenborg, J. Neutron-flux and gamma-dose distributions in the NPR shield. Nuclear Applications 2, No. 5: 430-439. 1966.
5. Hurwitz, A., Jr. Note on a theory of minimum weight shields. The General Electric Company, Knolls Atomic Power Lab. Report KAPL-1441 [Schenectady, N.Y.] 1957.
6. Murray, R. L. Nuclear reactor physics. Englewood Cliffs, N.J., Prentice-Hall Inc. 1957.
7. Mynatt, F. R. and Engle, W. W., Jr. Development of one-dimensional shield optimization techniques. Neutron Physics Division Annual Progress Report ORNL-4280: 61-62 [Oak Ridge National Lab., Tenn.] 1968.
8. Mynatt, F. R., Williams, L. R., Claibirne, H. C., Ford, W. E., III and Solomite, J. M. The discrete ordinate method-shielding applications. Neutron Physics Division Annual Progress Report ORNL-4134: 53-56 [Oak Ridge National Lab., Tenn.] 1967.
9. Pfeiffer, W. and Shapiro, J. Applications of a macroscopic formulation of transport theory. Nuclear Science and Engineering 34, No. 3: 336-339. 1968.
10. Sasse, S. Weight optimization for radiation shields of large reactors. U.S. Atomic Energy Commission Report ORNL-TR-1525 [Oak Ridge National Lab., Tenn.] 1967.
11. Smith, W. R. and Turner, M. A. Nuclear merchant ship reactor shield design summary report. Babcock and Wilcox Company, Atomic Energy Division Report BAW-1144-1 [Lynchburg, Va.] 1959.

12. Troubetzkoy, E. S. Minimum weight shield synthesis. United Nuclear Corp., Development Division-NDA Report UNC-5017 (Part A) [White Plains, N.Y.] 1962.
13. U.S. Atomic Energy Commission. Reactor physics constants. U.S. Atomic Energy Commission Report ANL-5800 [Argonne National Lab., Lemont, Ill.] 1963.
14. Yarmush, D., Zell, J. and Aronson, R. The transmission matrix method for penetration problems. Wright Air Development Center Technical Report: 59-772. 1960.

ACKNOWLEDGMENTS

The author wishes to express his gratitude to Dr. Alfred Rohach for his guidance and assistance in this investigation. The author wishes to thank Drs. Glenn Murphy, William Gorman III, Richard Seagrave and Paul Barcus who, along with Dr. Rohach, formed his graduate committee.

The author wishes to thank the National Aeronautics and Space Administration for the fellowship under which this work was done.

Finally, the author extends his deepest gratitude to his wife Nancy for her continuous understanding and patience.